Vaccination boosts naturally enhanced neutralizing breadth to SARS-CoV-2 one year after infection

Zijun Wang[1,*], Frauke Muecksch[2,*], Dennis Schaefer-Babajew[1,*], Shlomo Finkin[1,*], Charlotte Viant[1,*], Christian Gaebler[1,*], Christopher Barnes[3], Melissa Cipolla[1], Victor Ramos[1], Thiago Y. Oliveira[1], Alice Cho[1], Fabian Schmidt[2], Justin da Silva[2], Eva Bednarski[2], Mridushi Daga[1], Martina Turroja[1], Katrina G. Millard[1], Mila Jankovic[1], Anna Gazumyan[1, 4], Paul D. Bieniasz[2, 4], Marina Caskey[1], Theodora Hatziioannou[2] and Michel C. Nussenzweig[1, 4]

[1]Laboratory of Molecular Immunology, The Rockefeller University, New York, NY 10065, USA

[2]Laboratory of Retrovirology, The Rockefeller University, New York, NY 10065, USA

[3]Division of Biology and Biological Engineering, California Institute of Technology, Pasadena, CA, USA.

[4]Howard Hughes Medical Institute

*equal contribution

Address correspondence to: Paul D. Bieniasz pbieniasz@rockefeller.edu; Marina Caskey mcaskey@rockefeller.edu; Theodora Hatziioannou thatziio@rockefeller.edu; or Michel C. Nussenzweig nussen@rockefeller.edu

24

25 **Over one year after its inception, the coronavirus disease-2019 (COVID-19) pandemic**
26 **caused by severe acute respiratory syndrome coronavirus-2 (SARS-CoV-2) remains**
27 **difficult to control despite the availability of several excellent vaccines. Progress in**
28 **controlling the pandemic is slowed by the emergence of variants that appear to be more**
29 **transmissible and more resistant to antibodies[1,2]. Here we report on a cohort of 63 COVID-**
30 **19-convalescent individuals assessed at 1.3, 6.2 and 12 months after infection, 41% of**
31 **whom also received mRNA vaccines[3,4]. In the absence of vaccination antibody reactivity to**
32 **the receptor binding domain (RBD) of SARS-CoV-2, neutralizing activity and the number**
33 **of RBD-specific memory B cells remain relatively stable from 6 to 12 months. Vaccination**
34 **increases all components of the humoral response, and as expected, results in serum**
35 **neutralizing activities against variants of concern that are comparable to or greater than**
36 **neutralizing activity against the original Wuhan Hu-1 achieved by vaccination of naïve**
37 **individuals[2,5-8]. The mechanism underlying these broad-based responses involves ongoing**
38 **antibody somatic mutation, memory B cell clonal turnover, and development of**
39 **monoclonal antibodies that are exceptionally resistant to SARS-CoV-2 RBD mutations,**
40 **including those found in variants of concern[4,9]. In addition, B cell clones expressing broad**
41 **and potent antibodies are selectively retained in the repertoire over time and expand**
42 **dramatically after vaccination. The data suggest that immunity in convalescent individuals**
43 **will be very long lasting and that convalescent individuals who receive available mRNA**
44 **vaccines will produce antibodies and memory B cells that should be protective against**
45 **circulating SARS-CoV-2 variants. Should memory responses evolve in a similar manner in**

46 **vaccinated individuals, additional appropriately timed boosting with available vaccines**
47 **could cover most circulating variants of concern.**
48
49 We initially characterized immune responses to SARS-CoV-2 in a cohort of convalescent
50 individuals 1.3 and 6.2 months after infection[3,4]. Between February 8 and March 26, 2021, 63
51 participants returned for a 12-month follow-up visit among whom 26 (41%) had received at least
52 one dose of either the Moderna (mRNA-1273) or Pfizer-BioNTech (BNT162b2) vaccines, on
53 average 40 days before their study visit (Supplementary Table 1). Of the individuals that
54 returned for a 12-month follow-up, 10% had been hospitalized and the remainder had
55 experienced relatively mild initial infections. Only 14% of the individuals reported persistent
56 long-term symptoms after 12 months, reduced from 44% at the 6-month time point[4]. Symptom
57 persistence was not associated with the duration and severity of acute disease or with vaccination
58 status (Extended Data Fig. 1 a-c). All participants tested negative for active infection at the 12-
59 month time point as measured by a saliva-based PCR assay [4]. The demographics and clinical
60 characteristics of the participants are shown in Supplementary Tables 1 and 2.
61
62 **Plasma SARS-CoV-2 Antibody Reactivity**
63 Antibody reactivity in plasma to the RBD and nucleoprotein (N) were measured by enzyme-
64 linked immunosorbent assay (ELISA)[3]. Convalescent participants who had not been vaccinated
65 maintained most of their anti-RBD IgM (103%), IgG (88%), and IgA (72%) titers between 6 and
66 12 months (Fig. 1a and Extended Data Fig. 2a-h). Consistent with previous reports[5-8],
67 vaccination increased the anti-RBD plasma antibody levels, with IgG titers increasing by nearly
68 5-fold compared to unvaccinated individuals (Fig. 1a right). The 2 individuals who did not show

69 an increase had been vaccinated only 2 days before sample collection. In contrast to anti-RBD
70 antibody titers that were relatively stable, anti-N antibody titers decreased significantly between
71 6 and 12 months irrespective of vaccination (Fig. 1b). Thus, persistence of humoral immunity to
72 individual SARS-CoV-2 viral antigens differs, favoring longevity of anti-RBD over anti-N
73 responses.
74
75 Plasma neutralizing activity in 63 participants was measured using an HIV-1 pseudotyped with
76 the SARS-CoV-2 spike protein [3,4,10] (Fig. 1c-e). Twelve-months after infection, the geometric
77 mean half-maximal neutralizing titer (NT_{50}) for the 37 individuals that had not been vaccinated
78 was 75, which was not significantly different from the same individuals at 6.2 months (Fig. 1d).
79 In contrast, the vaccinated individuals showed a geometric mean NT_{50} of 3,684, which was
80 nearly 50-fold greater than unvaccinated individuals and disproportionately increased compared
81 to anti-RBD IgG antibodies (Fig. 1a, d, and e). Neutralizing activity was directly correlated with
82 IgG anti-RBD (Extended Data Fig.2i) but not with anti-N titers (Extended Data Fig.2k). We
83 conclude that neutralizing titers remain relatively unchanged between 6 to 12 months after
84 SARS-CoV-2 infection, and that vaccination further boosts this activity by nearly 50-fold.
85
86 To determine the neutralizing activity against circulating variants of concern/interest, we
87 performed neutralization assays on HIV-1 virus pseudotyped with the S protein of the following
88 SARS-CoV-2 variants of concern/interest: B.1.1.7, B.1.351, B.1.526 [1,11,12]. Twelve-months after
89 infection neutralizing activity against the variants was generally lower than against wild-type
90 SARS-CoV-2 virus in the same assay with the greatest loss of activity against B.1.351 (Fig. 1f).
91 After vaccination the geometric mean NT_{50} rose to 11,493, 48,341 and 22,109 against B.1.351,

92 B.1.1.7 and B.1.526, respectively. These titers are an order of magnitude higher than the
93 neutralizing titers achieved against the wild-type SARS-CoV-2 at the peak of the initial response
94 in infected individuals and in naïve individuals receiving both doses of mRNA vaccines (Fig. 1d
95 and [2,5-8]).
96
97 **Memory B cells**
98 The memory B cell compartment serves as an immune reservoir that contains a diverse collection
99 of antibodies[13,14]. To enumerate RBD-specific memory B cells, we performed flow cytometry
100 using a biotin-labeled RBD[3] (Fig. 2a upper panel, Extended Data Fig. 3a and b). In the absence
101 of vaccination, the number of RBD specific memory B cells present at 12 months was only 1.35-
102 fold lower than the earlier timepoint (p= 0.027, Fig. 2b). In contrast and consistent with previous
103 reports[5,8,15], convalescent individuals that received mRNA vaccines showed an average 8.6-fold
104 increase in the number of circulating RBD specific memory B cells (Fig. 2b). B cells expressing
105 antibodies that bound to both wild-type and K417N/E484K/N501Y mutant RBDs were also
106 enumerated by flow cytometry (Fig. 2a lower panel, Extended Data Fig 3c). The number of
107 variant RBD cross-reactive B cells was directly proportional to but 1.6 to 3.2-fold lower than
108 wild-type RBD binding B cells (Fig. 2b).
109
110 The memory B cell compartment accumulates mutations and undergoes clonal evolution over the
111 initial 6 months after infection[4,9,16,17]. To determine whether the memory compartment continues
112 to evolve between 6 and 12 months, we obtained 1105 paired antibody heavy and light chain
113 sequences from 10 individuals that were also assayed at the earlier time points, 6 of which were
114 vaccinated (Fig. 2c, Extended Data Fig 3d, Supplementary Table 3). There were few significant

differences among the expressed IGHV and IGLV genes between vaccinated and un-vaccinated groups, or between the 1.3-, 6-month and 1 year time points (Extended Data Fig 4a-c)[3,4]. *IGHV3-30* and *IGHV3-53* remained over-represented irrespective of vaccination [18,19](Extended Data Fig 4a).

All individuals assayed at 12 months showed expanded clones of RBD-binding memory cells that expressed closely related IGHV and IGLV genes (Fig.2c and d, Extended Data Fig 3d). The relative fraction of cells belonging to these clones varied from 7-54% of the repertoire with no significant difference between vaccinated and non-vaccinated groups. The overall clonal composition differed between 6 and 12 months in all individuals suggesting ongoing clonal evolution (Fig. 2c, Extended Data Fig 3d). Among the 89 clones found after 12 months, 61% were not previously detected and 39% were present at one of the earlier time points (Fig. 2c, Extended Data Fig 3d). In vaccinated individuals the increase in size of the memory compartment was paralleled by an increase in the absolute number of B cells representing all persistent clones (Fig. 2b and e, Extended Data Fig 5a). Thus, RBD specific memory B cell clones were re-expanded upon vaccination in all 6 convalescent individuals examined (Fig. 2c and e, Extended Data Fig 3d and Extended Data Fig 5a).

Somatic hypermutation of antibody genes continued between 6 and 12 months after infection (Fig. 2f). Slightly higher levels of mutation were found in individuals who had not been vaccinated compared to vaccinated individuals possibly due to recruitment of newly-formed memory cells into the expanded memory compartment of the vaccinated individuals (Fig. 2c-e, Extended Data Fig 5b). There was no significant difference in mutation between conserved and

138 newly arising clones at the 12-month time point in vaccinated individuals (Extended Data Fig
139 5c). Moreover, phylogenetic analysis revealed that sequences found at 6 and 12 months were
140 intermingled and similarly distant from their unmutated common ancestors (Extended Data Fig
141 6). We conclude that clonal re-expansion of memory cells in response to vaccination is not
142 associated with additional accumulation of large numbers of somatic mutations as might be
143 expected if the clones were re-entering and proliferating in germinal centers.
144

145 **Neutralizing Activity of Monoclonal Antibodies**

146 To determine whether the antibodies obtained from memory B cells 12 months after infection
147 bind to RBD we performed ELISAs (Fig.3a). 174 antibodies were tested by ELISA including: 1.
148 53 that were randomly selected from those that appeared only once and only after 1 year; 2. 91
149 that appeared as expanded clones or singlets at more than one time point; 3. 30 representatives of
150 newly arising expanded clones (Supplementary Tables 4 and 5). Among the 174 antibodies
151 tested, 173 bound to RBD indicating that the flow cytometry method used to identify B cells
152 expressing anti-RBD antibodies was efficient (Supplementary Tables 4 and 5). The geometric
153 mean ELISA half-maximal concentration (EC_{50}) of the antibodies obtained after 12 months was
154 2.6 ng/ml, which was significantly lower than at 6 months irrespective of vaccination and
155 suggestive of an increase in affinity (Fig. 3a, Extended data Fig. 7 a and b and Supplementary
156 Tables 4 and 5).
157

158 All 174 RBD binding antibodies obtained from the 12-month time point were tested for
159 neutralizing activity in a SARS-CoV-2 pseudotype neutralization assay. When compared to the
160 earlier time points from the same individuals, the geometric mean half maximal inhibitory

161 concentration (IC_{50}) improved from 171 ng/mL (1.3 months) to 116 ng/mL (6 months) to 79
162 ng/mL (12 months), with no significant difference between vaccinated and non-vaccinated
163 individuals (Fig. 3b and Extended data Fig. 7c, Supplementary Table 4). The increased potency
164 was especially evident in the antibodies expressed by expanded clones of B cells that were
165 conserved for the entire observation period irrespective of vaccination (p=0.014, Fig. 3b right
166 and c, Extended Data Fig 7e and Supplementary Table 5). The overall increase in neutralizing
167 activity among conserved clones was due to accumulation of clones expressing antibodies with
168 potent neutralizing activity and simultaneous loss of clones expressing antibodies with no
169 measurable activity (p= 0.028, Fig 3b right pie charts). Consistent with this observation,
170 antibodies obtained from clonally expanded B cells after 12 months were more potent than
171 antibodies obtained from unique B cells at the same time point (p= 0.029, Fig 3b).
172
173 **Epitopes and Breadth of Neutralization**
174 To determine whether the loss of non-neutralizing antibodies over time was due to preferential
175 loss of antibodies targeting specific epitopes, we performed BLI experiments in which a
176 preformed antibody-RBD complex was exposed to a second monoclonal targeting one of 3
177 classes of structurally defined epitopes[3,20] (see schematic in Fig. 4a). We assayed 60 randomly
178 selected antibodies with comparable neutralizing activity from the 1.3- and 12-month time
179 points. The 60 antibodies were evenly distributed between the 2 time points and between
180 neutralizers and non-neutralizers (Fig. 4). Antibody affinities for RBD were similar among
181 neutralizers and non-neutralizers obtained at the same time point (Fig. 4b, Extended Data Figure
182 8). Although the differences were small, both neutralizers and non-neutralizers showed increased
183 affinity over time (Fig. 4b, Extended Data Fig. 8). In competition experiments, all but 2 of the

184 30 non-neutralizing antibodies failed to inhibit binding of the class 1 (C105), 2 (C121 and C144)
185 or 3 (C135) antibodies tested and therefore must bind to epitopes that do not overlap with the
186 epitopes of these classes of antibodies (Fig. 4c, and Extended Data Fig. 9). In contrast, all but 2
187 of the 30 neutralizers blocked class 1, or 2 antibodies whose target epitopes are structural
188 components of the RBD that interact with its cellular receptor, the angiotensin-converting
189 enzyme 2[20,21] (ACE2) (Fig. 4c and Extended Data Fig. 9). In addition, whereas 9 of the 15
190 neutralizing antibodies obtained after 1.3 months blocked both class 1 and 2 antibodies, only 1 of
191 the 15 obtained after 12 months did so. In contrast to the earlier time point, 13 of 15 neutralizing
192 antibodies obtained after 12 months only interfered with C121, a class 2 antibody[3,20] (Fig. 4c and
193 Extended Data Fig. 9). We conclude that neutralizing antibodies are retained and non-
194 neutralizing antibodies targeting RBD surfaces that do not interact with ACE2 are removed from
195 the repertoire over time.
196
197 To determine whether there was an increase in neutralization breadth over time, the neutralizing
198 activity of the 60 antibodies was assayed against a panel of RBD mutants covering residues
199 associated with circulating variants of concern: R346S, K417N, N440K, A475V, E484K and
200 N501Y (Fig. 4d and Supplementary Table 6). Increased activity was evident against K417N,
201 N440K, A475V, E484K and N501Y (Fig. 4d and Supplementary Table 6). We conclude that
202 evolution of the antibody repertoire results in acquisition of neutralization breadth over time.
203
204 The increase in breadth and overall potency of memory B cell antibodies could be due to shifts in
205 the repertoire, clonal evolution, or both. To determine whether changes in specific clones are
206 associated with increases in affinity and breadth, we measured the relative affinity and

207 neutralizing breadth of pairs of antibodies expressed by expanded clones of B cells that were
208 maintained in the repertoire over the entire observation period[3,4]. SARS-CoV-2 neutralizing
209 activity was not significantly correlated with affinity at either time point considered
210 independently (Fig. 5a). However, there was a significant increase in overall affinity over time
211 including in the 4 pairs of antibodies with no measurable neutralizing activity (Fig 5b and
212 Supplementary Table 7). Neutralizing breadth was assayed for 15 randomly selected pairs of
213 antibodies targeting epitopes assigned to the 3 dominant classes of neutralizing
214 antibodies[3,20,22,23]. Seven of the selected antibodies showed equivalent or decreased activity
215 against wild-type SARS-CoV-2 after 12 months (Fig. 5c and Supplementary Table 8). However,
216 neutralizing breadth increased between 1.3 and 12-months for all 15 pairs, even when
217 neutralizing activity against the wild-type was unchanged or decreased (Fig. 5c and
218 Supplementary Table 8). Only 1 of the 15 antibodies obtained after 1.3 months neutralized all the
219 mutants tested (Fig. 5c). In contrast, 10 of the 15 antibodies obtained from the same clones after
220 12 months neutralized all variants tested with IC_{50}s as low as 1 ng/ml against the triple mutant
221 K417N/E484K/N501Y found in B.1.351 (Fig. 5c and Supplementary Table 8). In conclusion,
222 continued clonal evolution of anti-SARS-CoV-2 antibodies over 12 months favors increasing
223 potency and breadth resulting in monoclonal antibodies with exceptional activity against a broad
224 group of variants.
225
226 **Discussion**
227 During immune responses activated B cells interact with cognate T cells and begin dividing
228 before selection into the plasma cell, memory or germinal center B cell compartments based in
229 part on their affinity for antigen[14,24-28]. Whereas B cells expressing high affinity antibodies are

230 favored to enter the long-lived plasma cell compartment, the memory compartment is more
231 diverse and can develop directly from activated B cells or from a germinal center[14,24-28].
232 Memory cells emanating from a germinal center carry more mutations than those that develop
233 directly from activated B cells because they undergo additional cycles of division[29].
234
235 Consistent with the longevity of bone marrow plasma cells, infection with SARS-CoV-2 leads to
236 persistent serum anti-RBD antibodies, and corresponding neutralizing responses. Nearly 93% of
237 the plasma neutralizing activity is retained between 6- and 12-months[30,31]. Vaccination boosts the
238 neutralizing response by 1.5 orders of magnitude by inducing additional plasma cell
239 differentiation from the memory B cell compartment [32]. Recruitment of evolved memory B cells
240 producing antibodies with broad and potent neutralizing activity into the plasma cell
241 compartment is likely to account for the exceptional serologic activity of vaccinated
242 convalescents against variants of concern[15,32,33].
243
244 Less is known about selection and maintenance of the memory B cell compartment. SARS-CoV-
245 2 infection produces a memory compartment that continues to evolve over 12 months after
246 infection with accumulation of somatic mutations, emergence of new clones, and increasing
247 affinity all of which is consistent with long-term persistence of germinal centers. The increase in
248 activity against SARS-CoV-2 mutants parallels the increase in affinity and is consistent with the
249 finding that increasing the apparent affinity of anti-SARS-2 antibodies by dimerization or by
250 creating bi-specific antibodies also increases resistance to RBD mutations[34-37].
251

252 Continued antibody evolution in germinal centers requires antigen which can be retained in these
253 structures over long periods of time[26]. In addition, SARS-CoV-2 protein and nucleic acid has
254 been reported in the gut for at least 2 months after infection[4]. Irrespective of the source of
255 antigen, antibody evolution favors epitopes overlapping with the ACE2 binding site on the RBD,
256 possibly because these are epitopes that are preferentially exposed on trimeric spike protein or
257 virus particles.
258
259 Vaccination after SARS-CoV-2 infection increases the number of RBD binding memory cells by
260 over an order of magnitude by recruiting new B cell clones into memory and expanding
261 persistent clones. The persistent clones expand without accumulating large numbers of additional
262 mutations indicating that clonal expansion of human memory B cells does not require re-entry
263 into germinal centers and occurs through the activated B cell compartment[14,24-28].
264
265 The remarkable evolution of breadth after infection and the robust enhancement of serologic
266 responses and B cell memory achieved with mRNA vaccination suggests that convalescent
267 individuals who are vaccinated should enjoy high levels of protection against emerging variants
268 without a need to modify existing vaccines. If memory responses evolve in a similar manner in
269 naive individuals that receive vaccines, additional appropriately timed boosting with available
270 vaccines should lead to protective immunity against circulating variants.
271
272
273
274

275 **Figures**

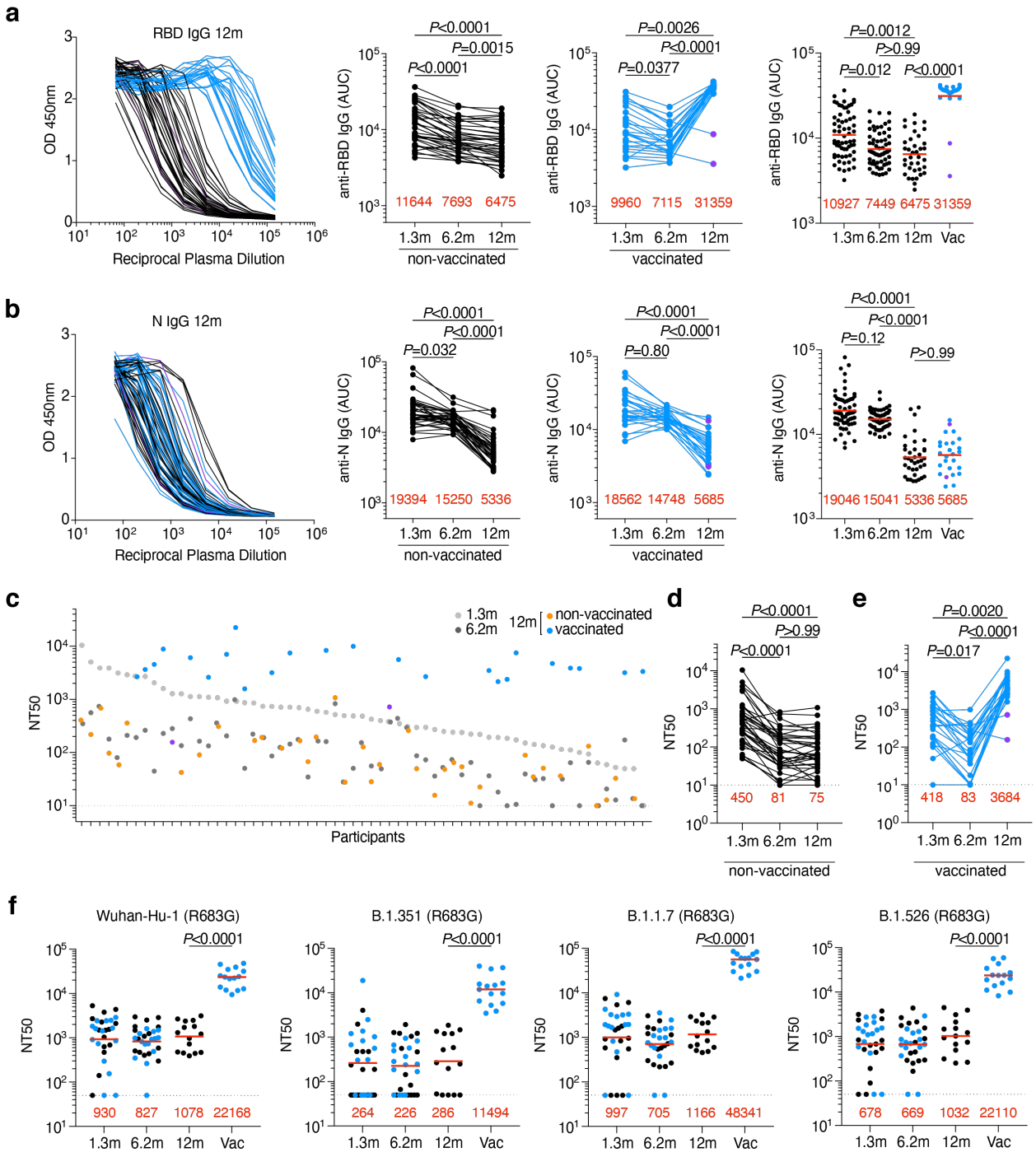

276

277

278 **Fig. 1: Plasma ELISAs and neutralizing activity. a-b,** Plasma IgG antibody binding to SARS-

279 CoV-2 RBD (**a**) and N protein (**b**), and plasma neutralizing activity (**c**–**e**) 12 months after infection

280 (N=63). **a** and **b**, ELISA curves from non-vaccinated (black lines) individuals, as well as
281 individuals who received one or two doses of a COVID-19 mRNA vaccine (blue lines),
282 respectively (left panels). Area under the curve (AUC) over time in non-vaccinated and vaccinated
283 individuals, as indicated (middle panels). Two individuals who received their first dose of vaccine
284 24-48 hours before sample collection are depicted in purple. Lines connect longitudinal samples.
285 Numbers in red indicate geometric mean AUC at the indicated timepoint. Right most panel shows
286 combined values as a dot plot for all individuals. **c**, ranked average NT50 at 1.3 months (light grey)
287 and 6.2 months (dark grey), as well as at 12 months for non-vaccinated (orange) individuals, and
288 individuals who received one or two doses (blue circles) of a COVID-19 mRNA vaccine,
289 respectively. Two individuals who received their first dose of vaccine 24-48 hours before sample
290 collection are depicted in purple. **d, e,** NT50 over time in non-vaccinated (**d**) and vaccinated
291 individuals (**e**). Lines connect longitudinal samples from the same individual. Two individuals
292 who received their first dose of vaccine 24-48 hours before sample collection are depicted in
293 purple. Red numbers indicate the geometric mean NT50 at the indicated timepoint. Statistical
294 significance in **a, b, d** and **e** was determined using Friedman Multiple Comparisons test. **f**, Plasma
295 neutralizing activity against SARS-CoV-2 variants of concern. All experiments were performed at
296 least in duplicate.
297

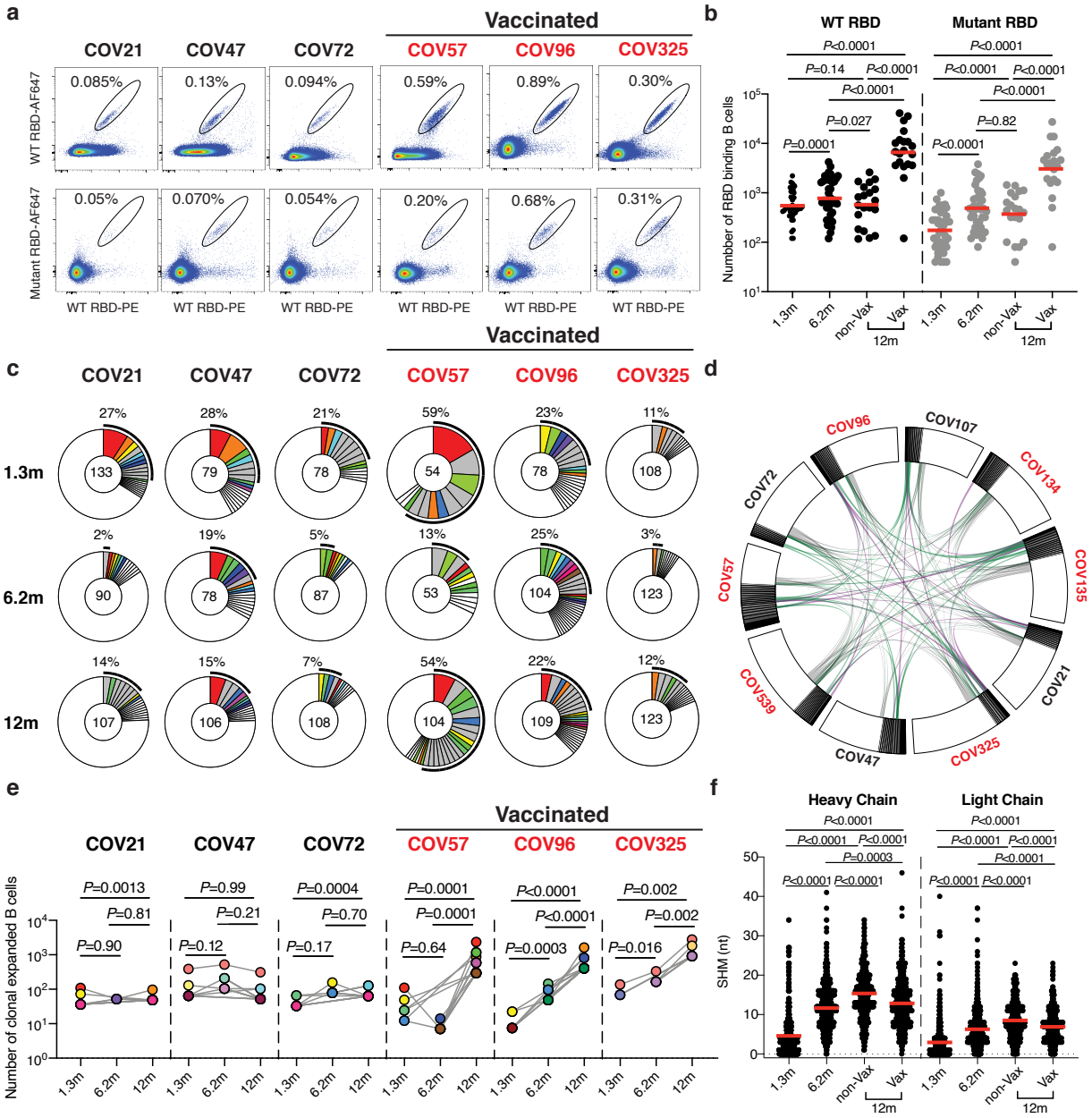
a
Vaccinated
COV21
COV47
COV72
COV57
COV96
COV325
WT RBD-AF647
Mutant RBD-AF647
0.085%
0.13%
0.094%
0.59%
0.89%
0.30%
0.05%
0.070%
0.054%
0.20%
0.68%
0.31%
WT RBD-PE
b
WT RBD
Mutant RBD
Numbber of RBD binding B cells
1.3m
6.2m
non-Vax
Vax
12m
c
1.3m
6.2m
12m
27%
28%
21%
59%
23%
11%
133
79
78
54
78
108
2%
19%
5%
13%
25%
3%
90
78
87
53
104
123
14%
15%
7%
54%
22%
12%
107
106
108
104
109
123
d
COV96
COV107
COV134
COV72
COV135
COV57
COV21
COV539
COV47
COV325
e
Number of clonal expanded B cells
P=0.0013
P=0.81
P=0.90
P=0.99
P=0.21
P=0.12
P=0.0004
P=0.70
P=0.17
P=0.0001
P=0.0001
P=0.64
P<0.0001
P<0.0001
P=0.0003
P=0.002
P=0.002
P=0.016
f
Heavy Chain
Light Chain
SHM (nt)

298

299

300 **Fig. 2: Anti-SARS-CoV-2 RBD B cell memory. a,** Representative flow cytometry plots showing
301 dual AlexaFluor-647-RBD WT, or AlexaFluor-647-K417N/E484K/N501Y mutant and PE-RBD-
302 binding B cells for 6 individuals. Vaccine recipients are indicated in red. Gating strategy is found
303 in Extended Data Fig. 3a. Percentage of antigen-specific B cells is indicated. **b.** As in **a.** graph
304 summarizes number of antigen binding memory B cells per 2 million B cells (Extended data Fig
305 5b and c) obtained at 1.3, 6.2 and 12 months from 40 randomly selected individuals (vaccinees
306 n=20, and non-vaccinees, n=20). Each dot is one individual. Red horizontal bars indicate geometric
307 mean values. Statistical significance was determined using two-tailed Mann–Whitney U-tests. **c,**
308 Pie charts show the distribution of antibody sequences from 6 individuals after 1.3 [3] (upper panel)
309 or 6.2 [4] (middle panel) or 12 months (lower panel). The number in the inner circle indicates the
310 number of sequences analyzed for the individual denoted above the circle. Pie slice size is
311 proportional to the number of clonally related sequences. The black outline indicates the frequency
312 of clonally expanded sequences detected in each participant. Colored slices indicate persisting
313 clones (same IGV and IGJ genes, with highly similar CDR3s) found at both timepoints in the same
314 participant. Grey slices indicate clones unique to the timepoint. White indicates sequences isolated
315 once, and white slices indicate singlets found at both timepoints. **d.** Circos plot depicts the
316 relationship between antibodies that share V and J gene segment sequences at both IGH and IGL.
317 Purple, green, and grey lines connect related clones, clones and singles, and singles to each other,
318 respectively. **e.** Number of clonally expanded B cells (per 10 million B cells) at indicated time
319 points in 6 individuals. Colors indicate shared clones appearing at different time points. Statistical
320 significance was determined using Wilcoxon matched-pairs signed rank test. Vaccinees are
321 marked in red. **f,** Number of somatic nucleotide mutations in the IGVH and IGVL in antibodies
322 (also Supplementary table 3) obtained after 1.3 or 6.2 or 12 months from 10 donors (vaccinees,

n=6, non-vaccinees, n=4). Red horizontal bars indicate mean values. Statistical significance was determined using two-tailed Mann–Whitney U-tests.

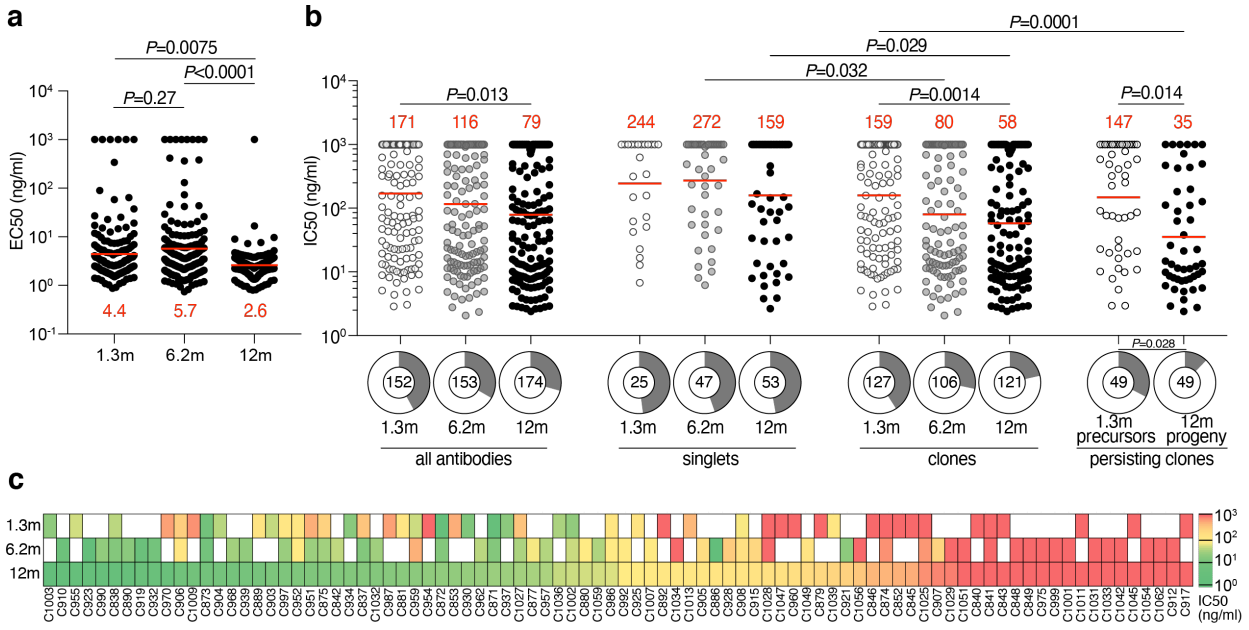

Fig. 3: Anti-SARS-CoV-2 RBD monoclonal antibodies. a, Graph shows the ELISA binding EC_{50} (Y axis) for SARS-CoV-2 RBD by antibodies isolated at 1.3[3] 6.2[4] and 12 months after infection. Statistical significance was determined using the Kruskal-Wallis test. **b-c,** Graphs show anti-SARS-CoV-2 neutralizing activity of monoclonal antibodies measured by a SARS-CoV-2 pseudovirus neutralization assay[3,10]. Half-maximal inhibitory concentration (IC_{50}) values for antibodies isolated at 1.3[3] 6.2[4] and 12 months after infection. **b**, Wild-type SARS-CoV-2 (Wuhan-Hu-1 strain[38]) neutralization by monoclonal antibodies. Each dot represents one antibody. Pie charts illustrate the fraction of non-neutralizing (IC50 > 1000 ng/ml) antibodies (grey slices), inner circle shows number of antibodies tested. Horizontal bars and red numbers indicate geometric mean values. Statistical significance was determined through the Kruskal Wallis test with subsequent Dunn's multiple comparisons. **c.** Heat map shows the neutralizing activity of clonally related antibodies against wt-SARS-CoV-2 over time. White tiles indicate no clonal relative at the respective time point. Clones are ranked from left to right by the potency of the 12-month progeny

340 antibodies which are denoted below the tiles. For **b** and **c**, antibodies with IC_{50} values above 1000

341 ng/ml were plotted at 1000 ng/ml. The average of two independent experiments is shown.

342

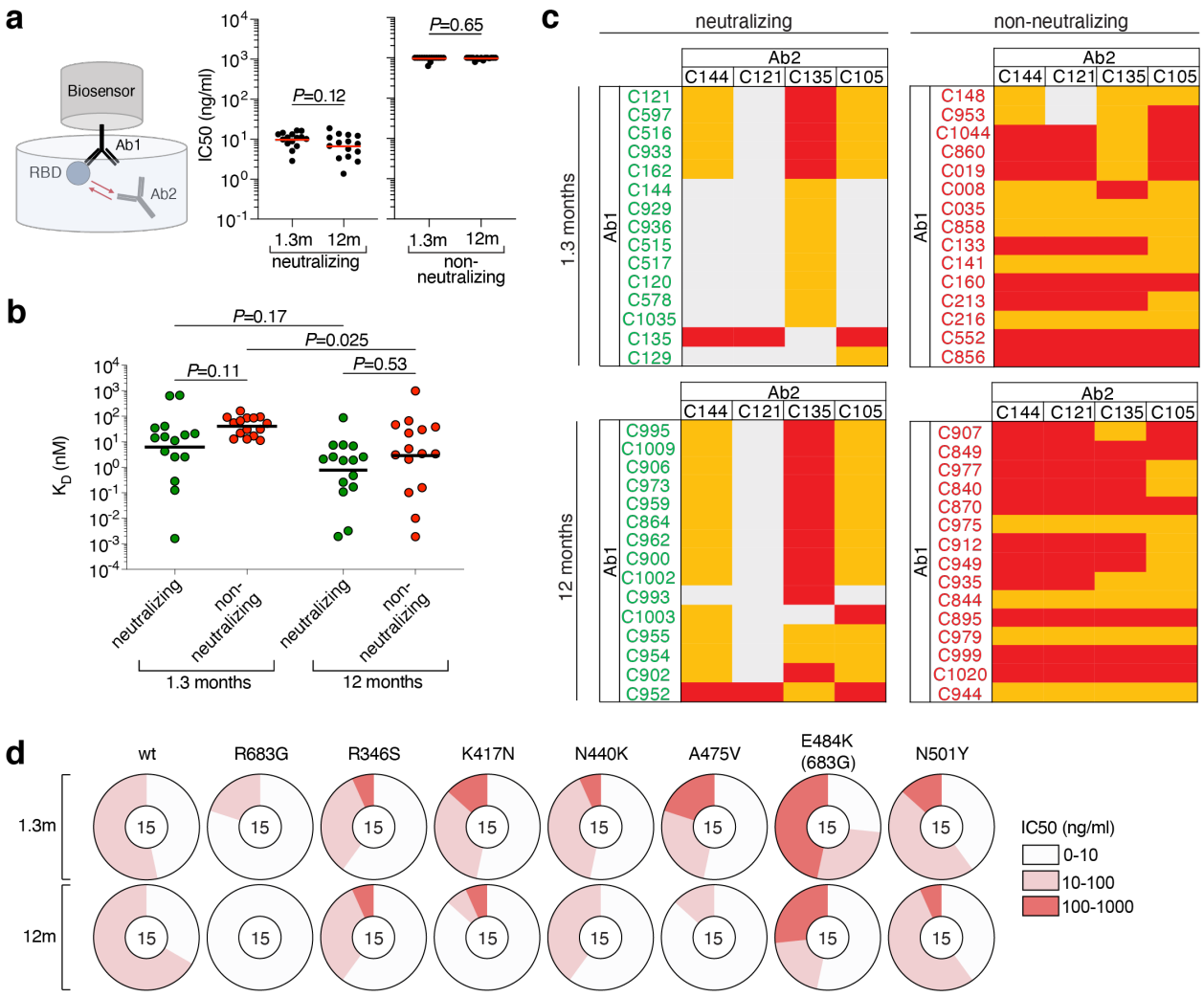

Fig. 4: Epitope targeting of anti-SARS-CoV-2 RBD antibodies. a, Schematic representation of the BLI experiment (left) and IC_{50} values for randomly selected neutralizing (middle) and non-neutralizing (right) antibodies isolated at 1.3- and 12-months post-infection. Red horizontal bars indicate geometric mean values. Statistical significance was determined using Mann-Whitney test. **b**, K_D values of the neutralizing (green) and non-neutralizing (red) antibodies isolated at 1.3 and 12 months after infection. Red horizontal bars indicate geometric mean values. Statistical significance was determined using Kruskal Wallis test with subsequent Dunn's multiple comparisons. BLI traces can be found in Extended data Fig. 8. **c,** Biolayer interferometry results

352 presented as a heat-map of relative inhibition of Ab2 binding to the preformed Ab1-RBD
353 complexes (grey=no binding, orange=intermediate binding, red=high binding). Values are
354 normalized through the subtraction of the autologous antibody control. BLI traces can be found in
355 Extended Data Fig 9. **d**, Neutralization of the indicated mutants for antibodies shown in panel **a-**
356 **c**. Pie charts illustrate the fraction of antibodies that are poorly/non-neutralizing (IC_{50} 100-1000
357 ng/ml, red), intermediate neutralizing (IC_{50} 10-100 ng/ml, pink) and potently neutralizing (IC_{50} 0-
358 10 ng/ml, white) for each mutant. Number in inner circle shows number of antibodies tested.
359

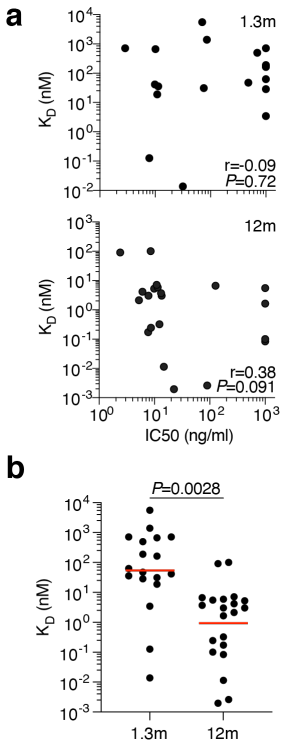

c

		ID	wt	R683G	R346S	K417N	N440K	A475V	E484K R683G	Q493R	N501Y	KEN R683G	Class
i	1.3m	C936	12	5	11	1000	12	152	10	13	1000	1000	1
	12m	C937	17	3	13	8	16	7	7	16	103	1000	
	1.3m	C517	11	3	8	1000	9	7	5	9	9	1000	
	12m	C1002	23	3	19	8	20	10	3	17	20	11	★
	1.3m	C933	20	12	15	24	17	28	1000	1000	54	1000	2
	12m	C934	11	5	11	9	9	10	1000	137	17	1000	
	1.3m	C129	10	1	8	2	6	6	1000	25	12	1000	
	12m	C1003	6	0.3	6	2	4	3	252	4	4	237	★
	1.3m	C144	4	1	3	2	2	3	1000	1000	3	1000	
	12m	C871	22	1	21	9	15	9	1000	6	14	1000	
	1.3m	C929	12	3	9	10	8	31	4	18	93	232	x
	12m	C930	22	2	17	3	16	6	3	13	10	16	★
ii	1.3m	C202	325	210	227	1000	235	1000	636	1000	1000	1000	1
	12m	C1027*	21	2	18	4	16	5	3	10	17	2	★
	1.3m	C006	481	167	231	337	289	1000	723	1000	1000	1000	
	12m	C837	16	0.3	12	3	9	5	1	8	4	20	★
	1.3m	C888	88	42	80	47	69	86	1000	109	88	1000	2
	12m	C889	13	1	11	3	9	4	23	8	9	46	★
	1.3m	C153	95	37	92	40	83	454	1000	232	125	1000	
	12m	C881*	20	0.4	15	6	13	5	1	15	14	1	★
	1.3m	C861	507	227	320	166	301	125	1000	1000	569	1000	
	12m	C853	23	1	17	8	17	12	1000	15	14	1000	
	1.3m	C1008	667	524	1000	1000	929	107	1000	661	876	1000	
	12m	C1009	9	2	7	3	6	5	24	6	7	19	★
	1.3m	C032	83	14	1000	23	1000	39	8	40	98	14	3
	12m	C952*	12	0.5	7	6	4	7	0.5	8	11	1	★
	1.3m	C108	971	217	1000	248	741	684	372	486	1000	847	
	12m	C951	15	2	1000	6	13	9	4	10	15	4	
iii	1.3m	C581	27	13	1000	8	23	22	71	26	34	21	3
	12m	C908	75	11	65	30	47	42	31	46	81	16	★

IC50 (ng/ml)

Fig. 5: Clonal evolution of anti-SARS-CoV-2 RBD antibodies. a, Graphs show affinities (Y axis) plotted against neutralization activity (X axis) for clonal antibody pairs isolated 1.3 (top) and 12 months (bottom) after infection. **b,** BLI affinity measurements for same paired 1.3- and 12-month antibodies as in **a**. **c,** IC_{50} values for 15 neutralizing antibody pairs against indicated mutant SARS-CoV-2 pseudoviruses. Antibodies are divided into groups i-iii, based on neutralizing activity: (i) potent clonal pairs that do not improve over time, (ii) clonal pairs that show increased activity over time, and (iii) and clonal pairs showing decreased neutralization activity after 12 months. Antibody class assignment based on initial (1.3m) sensitivity to mutation is indicated on the right. Red stars indicate antibodies that neutralize all RBD mutants tested. Color gradient indicates IC_{50} values ranging from 0 (white) to 1000 ng/ml (red).

373 **Methods**

374 **Study participants**.

375 Previously enrolled study participants were asked to return for a 12-month follow-up visit at the
376 Rockefeller University Hospital in New York from February 8 to March 26, 2021. Eligible
377 participants were adults with a history of participation in both prior study visits of our longitudinal
378 cohort study of COVID-19 recovered individuals[3,4]. All participants had a confirmed history of
379 SARS-CoV-2 infection, either diagnosed during the acute infection by RT-PCR or retrospectively
380 confirmed by seroconversion. Exclusion criteria included presence of symptoms suggestive of
381 active SARS-CoV-2 infection. Most study participants were residents of the Greater New York
382 City tri-state region and were asked to return approximately 12 months after the time of onset of
383 COVID-19 symptoms. Participants presented to the Rockefeller University Hospital for blood
384 sample collection and were asked about potential symptom persistence since their 6.2-month study
385 visit, laboratory-confirmed episodes of reinfection with SARS-CoV-2, and whether they had
386 received any COVID-19 related treatment or SARS-CoV-2 vaccination in the interim. Detailed
387 characteristics of the symptomology and severity of the acute infection, symptom kinetics, and the
388 immediate convalescent phase (7 weeks post-symptom onset until 6.2month visit) have been
389 reported previously [4]. Participants that presented with persistent symptoms attributable to COVID-
390 19 were identified on the basis of chronic shortness of breath or fatigue, deficit in athletic ability
391 and/or three or more additional long-term symptoms such as persistent unexplained fevers, chest
392 pain, new-onset cardiac sequalae, arthralgias, impairment of concentration/mental acuity,
393 impairment of sense of smell/taste, neuropathy or cutaneous findings as previously described [4].
394 All participants at Rockefeller University provided written informed consent before participation

395 in the study and the study was conducted in accordance with Good Clinical Practice. For detailed
396 participant characteristics see Supplementary Table 2.
397
398 **SARS-CoV-2 molecular tests**
399 Saliva was collected into guanidine thiocyanate buffer as described [39]. RNA was extracted using
400 either a column-based (Qiagen QIAmp DSP Viral RNA Mini Kit, Cat#61904) or a magnetic bead-
401 based method as described [40]. Reverse transcribed cDNA was amplified using primers and probes
402 validated by the CDC or by Columbia University Personalized Medicine Genomics Laboratory
403 respectively and approved by the FDA under the Emergency Use Authorization. Viral RNA was
404 considered detected if Ct for two viral primers/probes were <40.
405
406 **Blood samples processing and storage.**
407 Peripheral Blood Mononuclear Cells (PBMCs) obtained from samples collected at Rockefeller
408 University were purified as previously reported by gradient centrifugation and stored in liquid
409 nitrogen in the presence of FCS and DMSO [3,4]. Heparinized plasma and serum samples were
410 aliquoted and stored at -20 °C or less. Prior to experiments, aliquots of plasma samples were
411 heat-inactivated (56 °C for 1 hour) and then stored at 4 °C.
412
413 **ELISAs**
414 ELISAs[41,42] to evaluate antibodies binding to SARS-CoV-2 RBD and N were performed by
415 coating of high-binding 96-half-well plates (Corning 3690) with 50 µl per well of a 1µg/ml
416 protein solution in PBS overnight at 4 °C. Plates were washed 6 times with washing buffer (1×
417 PBS with 0.05% Tween-20 (Sigma-Aldrich)) and incubated with 170 µl per well blocking buffer

418 (1× PBS with 2% BSA and 0.05% Tween-20 (Sigma)) for 1 h at room temperature. Immediately
419 after blocking, monoclonal antibodies or plasma samples were added in PBS and incubated for 1
420 h at room temperature. Plasma samples were assayed at a 1:66 starting dilution and 7 additional
421 threefold serial dilutions. Monoclonal antibodies were tested at 10 μg/ml starting concentration
422 and 10 additional fourfold serial dilutions. Plates were washed 6 times with washing buffer and
423 then incubated with anti-human IgG, IgM or IgA secondary antibody conjugated to horseradish
424 peroxidase (HRP) (Jackson Immuno Research 109-036-088 109-035-129 and Sigma A0295) in
425 blocking buffer at a 1:5,000 dilution (IgM and IgG) or 1:3,000 dilution (IgA). Plates were
426 developed by addition of the HRP substrate, TMB (ThermoFisher) for 10 min (plasma samples)
427 or 4 minutes (monoclonal antibodies). The developing reaction was stopped by adding 50 μl 1 M
428 H_2SO_4 and absorbance was measured at 450 nm with an ELISA microplate reader (FluoStar
429 Omega, BMG Labtech) with Omega and Omega MARS software for analysis. For plasma
430 samples, a positive control (plasma from participant COV72, diluted 66.6-fold and seven
431 additional threefold serial dilutions in PBS) was added to every assay plate for validation. The
432 average of its signal was used for normalization of all of the other values on the same plate with
433 Excel software before calculating the area under the curve using Prism V9.1(GraphPad). For
434 monoclonal antibodies, the EC50 was determined using four-parameter nonlinear regression
435 (GraphPad Prism V9.1).
436
437 **Proteins**
438 Mammalian expression vectors encoding the RBDs of SARS-CoV-2 (GenBank MN985325.1; S
439 protein residues 319-539) or K417N, E484K, N501Y RBD mutants with an N-terminal human

440 IL-2 or Mu phosphatase signal peptide were previously described [43]. SARS-CoV-2 Nucleocapsid
441 protein (N) was purchased from Sino Biological (40588-V08B).
442
443 **SARS-CoV-2 pseudotyped reporter virus**
444 A panel of plasmids expressing RBD-mutant SARS-CoV-2 spike proteins in the context of
445 pSARS-CoV-2-S $_{\Delta 19}$ has been described previously [2,9,23]. Variant pseudoviruses resembling
446 variants of concern B.1.1.7 (first isolated in the UK), B.1.351 (first isolated in South-Africa) and
447 B.1.526 (first isolated in New York City) were generated by introduction of substitutions using
448 synthetic gene fragments (IDT) or overlap extension PCR mediated mutagenesis and Gibson
449 assembly. Specifically, the variant-specific deletions and substitutions introduced were:
450 B.1.1.7: ΔH69/V70, ΔY144, N501Y, A470D, D614G, P681H, T761I, S982A, D118H
451 B.1.351: D80A, D215G, L242H, R246I, K417N, E484K, N501Y, D614G, A701V
452 B.1.526: L5F, T95I, D253G, E484K, D614G, A701V.
453 The E484K and K417N/E484K/N501Y (KEN) substitution, as well as the deletions/substitutions
454 corresponding to variants of concern were incorporated into a spike protein that also includes the
455 R683G substitution, which disrupts the furin cleaveage site and increases particle infectivity.
456 Neutralizing activity against mutant pseudoviruses were compared to a wildtype SARS-CoV-2
457 spike sequence (NC_045512), carrying R683G where appropriate.
458 SARS-CoV-2 pseudotyped particles were generated as previously described [3,10]. Briefly, 293T
459 cells were transfected with pNL4-3ΔEnv-nanoluc and pSARS-CoV-2-$S_{\Delta 19}$, particles were
460 harvested 48 hpt, filtered and stored at -80°C.
461
462 **Pseudotyped virus neutralization assay**

463 Fourfold serially diluted plasma from COVID-19-convalescent individuals or monoclonal
464 antibodies were incubated with SARS-CoV-2 pseudotyped virus for 1 h at 37 °C. The mixture
465 was subsequently incubated with $293T_{Ace2}$ cells[3] (for comparisons of plasma or monoclonal
466 antibodies from convalescent individuals) or HT1080Ace2 cl14 cells[10] (for analyses involving
467 mutant/variant pseudovirus panels), as indicated, for 48h after which cells were washed with
468 PBS and lysed with Luciferase Cell Culture Lysis 5× reagent (Promega). Nanoluc Luciferase
469 activity in lysates was measured using the Nano-Glo Luciferase Assay System (Promega) with
470 the Glomax Navigator (Promega). The obtained relative luminescence units were normalized to
471 those derived from cells infected with SARS-CoV-2 pseudotyped virus in the absence of plasma
472 or monoclonal antibodies. The half-maximal neutralization titers for plasma (NT_{50}) or half-
473 maximal and 90% inhibitory concentrations for monoclonal antibodies (IC_{50} and IC_{90}) were
474 determined using four-parameter nonlinear regression (least squares regression method without
475 weighting; constraints: top=1, bottom=0) (GraphPad Prism).
476
477 **Biotinylation of viral protein for use in flow cytometry**
478 Purified and Avi-tagged SARS-CoV-2 RBD or SARS-CoV-2 RBD KEN mutant (K417N,
479 E484K, N501Y) was biotinylated using the Biotin-Protein Ligase-BIRA kit according to
480 manufacturer's instructions (Avidity) as described before [3]. Ovalbumin (Sigma, A5503-1G) was
481 biotinylated using the EZ-Link Sulfo-NHS-LC-Biotinylation kit according to the manufacturer's
482 instructions (Thermo Scientific). Biotinylated ovalbumin was conjugated to streptavidin-BV711
483 (BD biosciences, 563262) and RBD to streptavidin-PE (BD Biosciences, 554061) and
484 streptavidin-AF647 (Biolegend, 405237) [3].
485

486 **Flow cytometry and single cell sorting**

487 Single-cell sorting by flow cytometry was described previously [3]. Briefly, peripheral blood
488 mononuclear cells were enriched for B cells by negative selection using a pan-B-cell isolation kit
489 according to the manufacturer's instructions (Miltenyi Biotec, 130-101-638). The enriched B
490 cells were incubated in FACS buffer (1× PBS, 2% FCS, 1 mM EDTA) with the following anti-
491 human antibodies (all at 1:200 dilution): anti-CD20-PECy7 (BD Biosciences, 335793), anti-
492 CD3-APC-eFluro 780 (Invitrogen, 47-0037-41), anti-CD8-APC-eFluor 780 (Invitrogen, 47-
493 0086-42), anti-CD16-APC-eFluor 780 (Invitrogen, 47-0168-41), anti-CD14-APC-eFluor 780
494 (Invitrogen, 47-0149-42), as well as Zombie NIR (BioLegend, 423105) and fluorophore-labelled
495 RBD and ovalbumin (Ova) for 30 min on ice. Single CD3-CD8-CD14-CD16-CD20+Ova-RBD-
496 PE+RBD-AF647+ B cells were sorted into individual wells of 96-well plates containing 4 µl of
497 lysis buffer (0.5× PBS, 10 mM DTT, 3,000 units/ml RNasin Ribonuclease Inhibitors (Promega,
498 N2615) per well using a FACS Aria III and FACSDiva software (Becton Dickinson) for
499 acquisition and FlowJo for analysis. The sorted cells were frozen on dry ice, and then stored at
500 −80 °C or immediately used for subsequent RNA reverse transcription. For B cell phenotype
501 analysis, in addition to above antibodies, B cells were also stained with following anti-human
502 antibodies: anti-IgD-BV421 (Biolegend, 348226), anti-CD27-FITC (BD biosciences, 555440),
503 anti-CD19-BV605 (Biolegend, 302244), anti-CD71- PerCP-Cy5.5 (Biolegend, 334114), anti-
504 IgG-PECF594 (BD biosciences, 562538), anti-IgM-AF700 (Biolegend, 314538), anti-IgA-
505 Viogreen (Miltenyi Biotec, 130-113-481).

506

507 **Antibody sequencing, cloning and expression**

508 Antibodies were identified and sequenced as described previously [3]. In brief, RNA from single
509 cells was reverse-transcribed (SuperScript III Reverse Transcriptase, Invitrogen, 18080-044) and
510 the cDNA stored at −20 °C or used for subsequent amplification of the variable IGH, IGL and
511 IGK genes by nested PCR and Sanger sequencing. Sequence analysis was performed using
512 MacVector. Amplicons from the first PCR reaction were used as templates for sequence- and
513 ligation-independent cloning into antibody expression vectors. Recombinant monoclonal
514 antibodies were produced and purified as previously described [3].
515
516 **Biolayer interferometry**
517 Biolayer interferometry assays were performed as previously described [3]. Briefly, we used the
518 Octet Red instrument (ForteBio) at 30 °C with shaking at 1,000 r.p.m. Epitope-binding assays
519 were performed with protein A biosensor (ForteBio 18-5010), following the manufacturer's
520 protocol 'classical sandwich assay'. (1) Sensor check: sensors immersed 30 s in buffer alone
521 (kinetics buffer 10x ForteBio 18-1105 diluted 1x in PBS1x). (2) Capture first antibody: sensors
522 immersed 10 min with Ab1 at 30 µg/ml. (3) Baseline: sensors immersed 30 s in buffer alone. (4)
523 Blocking: sensors immersed 5 min with IgG isotype control at 50 µg/ml. (6) Antigen association:
524 sensors immersed 5 min with RBD at 100 µg/ml. (7) Baseline: sensors immersed 30 s in buffer
525 alone. (8) Association Ab2: sensors immersed 5 min with Ab2 at 30 µg/ml. Curve fitting was
526 performed using the Fortebio Octet Data analysis software (ForteBio). Affinity measurement of
527 anti-SARS-CoV-2 IgGs binding were corrected by subtracting the signal obtained from traces
528 performed with IgGs in the absence of WT RBD. The kinetic analysis using protein A biosensor
529 (ForteBio 18-5010) was performed as follows: (1) baseline: 60sec immersion in buffer. (2)
530 loading: 200sec immersion in a solution with IgGs 30 µg/ml. (3) baseline: 200sec immersion in

531 buffer. (4) Association: 300sec immersion in solution with WT RBD at 200, 100, 50 or 25 μg/ml
532 (5) dissociation: 600sec immersion in buffer. Curve fitting was performed using a fast 1:1
533 binding model and the Data analysis software (ForteBio). Mean K_D values were determined by
534 averaging all binding curves that matched the theoretical fit with an R^2 value ≥ 0.8.
535
536 **Computational analyses of antibody sequences**
537 Antibody sequences were trimmed based on quality and annotated using Igblastn v.1.14. with
538 IMGT domain delineation system. Annotation was performed systematically using Change-O
539 toolkit v.0.4.540 [44]. Heavy and light chains derived from the same cell were paired, and
540 clonotypes were assigned based on their V and J genes using in-house R and Perl scripts (Fig.
541 2d). All scripts and the data used to process antibody sequences are publicly available on GitHub
542 (https://github.com/stratust/igpipeline).
543
544 The frequency distributions of human V genes in anti-SARS-CoV-2 antibodies from this study
545 was compared to 131,284,220 IgH and IgL sequences generated by [45] and downloaded from
546 cAb-Rep[46], a database of human shared BCR clonotypes available at https://cab-
547 rep.c2b2.columbia.edu/. Based on the 91 distinct V genes that make up the 6902 analyzed
548 sequences from Ig repertoire of the 10 participants present in this study, we selected the IgH and
549 IgL sequences from the database that are partially coded by the same V genes and counted them
550 according to the constant region. The frequencies shown in (Extended data Fig. 4**)** are relative to
551 the source and isotype analyzed. We used the two-sided binomial test to check whether the
552 number of sequences belonging to a specific IgHV or IgLV gene in the repertoire is different
553 according to the frequency of the same IgV gene in the database. Adjusted p-values were

554 calculated using the false discovery rate (FDR) correction. Significant differences are denoted
555 with stars.
556
557 Nucleotide somatic hypermutation and CDR3 length were determined using in-house R and Perl
558 scripts. For somatic hypermutations, IGHV and IGLV nucleotide sequences were aligned against
559 their closest germlines using Igblastn and the number of differences were considered nucleotide
560 mutations. The average mutations for V genes were calculated by dividing the sum of all
561 nucleotide mutations across all participants by the number of sequences used for the analysis. To
562 calculate the GRAVY scores of hydrophobicity [47] we used Guy H.R. Hydrophobicity scale based
563 on free energy of transfer (kcal/mole) [48] implemented by the R package Peptides (the
564 Comprehensive R Archive Network repository; https://journal.r-project.org/archive/2015/RJ-
565 2015-001/RJ-2015-001.pdf). We used 2680 heavy chain CDR3 amino acid sequences from this
566 study and 22,654,256 IGH CDR3 sequences from the public database of memory B cell receptor
567 sequences [49]. The two-tailed Wilcoxon matched-pairs signed rank test was used to test whether
568 there is a difference in hydrophobicity distribution.
569
570 Immunoglobulins grouped into the same clonal lineage had their respective IgH and IgL sequences
571 merged and subsequently aligned, using TranslatorX [50], with the unmutated ancestral sequence
572 obtained from IMGT/V-QUEST reference directory [51]. GCTree [52] was further used to perform the
573 phylogenetic trees construction. Each node represents a unique IgH and IgL combination and the
574 size of each node is proportional to the number of identical sequences. The numbered nodes
575 represent the unobserved ancestral genotypes between the germline sequence and the sequences
576 on the downstream branch.

Competing interests: The Rockefeller University has filed a provisional patent application in connection with this work on which M.C.N.is an inventor (US patent 63/021,387). The patent has been licensed by Rockefeller University to Bristol Meyers Squib.

Data availability statement: Data are provided in SI Tables 1-8. The raw sequencing data and computer scripts associated with Figure 2 have been deposited at Github (https://github.com/stratust/igpipeline). This study also uses data from "A Public Database of Memory and Naive B-Cell Receptor Sequences" (https://doi.org/10.5061/dryad.35ks2), PDB (6VYB and 6NB6) and from "High frequency of shared clonotypes in human B cell receptor repertoires" (https://doi.org/10.1038/s41586-019-0934-8).

Code availability statement: Computer code to process the antibody sequences is available at GitHub (https://github.com/stratust/igpipeline).

Data presentation

Figures arranged in Adobe Illustrator 2020.

Acknowledgements: We thank all study participants who devoted time to our research; The Rockefeller University Hospital nursing staff and Clinical Research Support Office and nursing staff. Mayu Okawa Frank, Marissa Bergh, and Robert B. Darnell for SARS-CoV-2 saliva PCR testing. Charles M. Rice, Pamela J. Bjorkman and all members of the M.C.N. laboratory for helpful discussions and Maša Jankovic for laboratory support. This work was supported by NIH grant P01-AI138398-S1 (M.C.N.) and 2U19AI111825 (M.C.N.). R37-AI64003 to P.D.B.; R01AI78788

601 to T.H.; We thank Dr. Jost Vielmetter and the Protein Expression Center in the Beckman Institute
602 at Caltech for expression assistance. C.O.B. is supported by the HHMI Hanna Gray and Burroughs
603 Wellcome PDEP fellowships. C.G. was supported by the Robert S. Wennett Post-Doctoral
604 Fellowship, in part by the National Center for Advancing Translational Sciences (National
605 Institutes of Health Clinical and Translational Science Award program, grant UL1 TR001866),
606 and by the Shapiro-Silverberg Fund for the Advancement of Translational Research. P.D.B. and
607 M.C.N. are Howard Hughes Medical Institute Investigators.
608
609 **Author Contributions:** P.D.B., T.H., and M.C.N. conceived, designed and analyzed the
610 experiments. M. Caskey and C.G. designed clinical protocols. Z.W., F.M., D.S.B., S.F., C.V.,
611 J.D.S., E.B., C.O.B., F.S., A.C., and M.J. carried out experiments. A.G. and M. Cipolla produced
612 antibodies. D.S.B., M.D., M.T., K.G.M., C.G. and M. Caskey recruited participants, executed
613 clinical protocols and processed samples. T.Y.O. and V.R. performed bioinformatic analysis.
614 Z.W., F.M, D.S.B., C.G. and M.C.N. wrote the manuscript with input from all co-authors.
615
616
617
618
619
620
621
622
623 **Extended Data Figures**

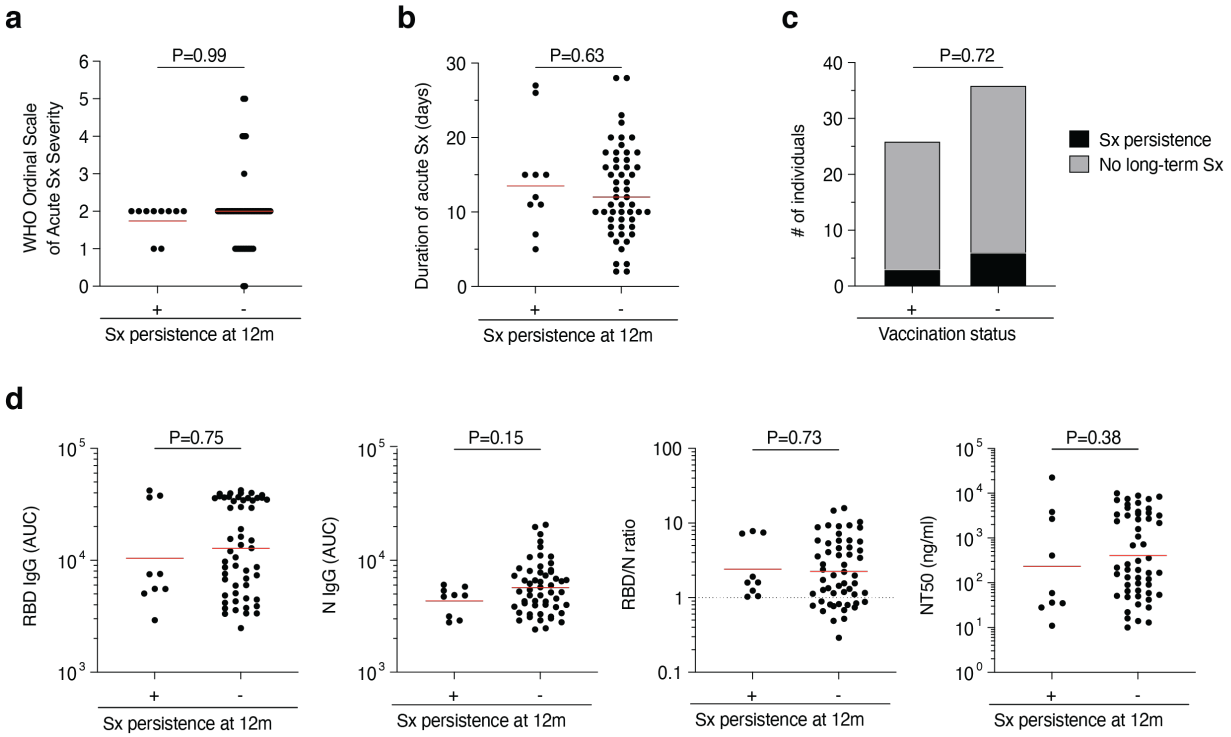

Extended Data Fig. 1 Clinical correlations. a-d, Association of persistence of symptoms (Sx) 12 months after infection with various clinical and serological parameters. **a-b,** Acute disease severity as assessed with the WHO Ordinal Scale of Clinical Improvement (**a**) and duration of acute phase symptoms (**b**) in individuals reporting persistent symptoms (+) compared to individuals who are symptom-free (-) 12 months post-infection. **c,** Proportion of individuals reporting persistent symptoms (black area) compared to individuals who are symptom-free (grey area) 12 months after infection grouped by vaccination status. **d,** Anti-RBD IgG, anti-N IgG, NT50 titers as well as the RBD/N IgG ratio at 12 months after infection in individuals reporting persistent symptoms (+) compared to individuals who are symptom-free (-) 12 months post-infection. Statistical significance was determined using the Mann-Whitney test in **a, b** and **d**, and using the Fisher's exact test in **c**.

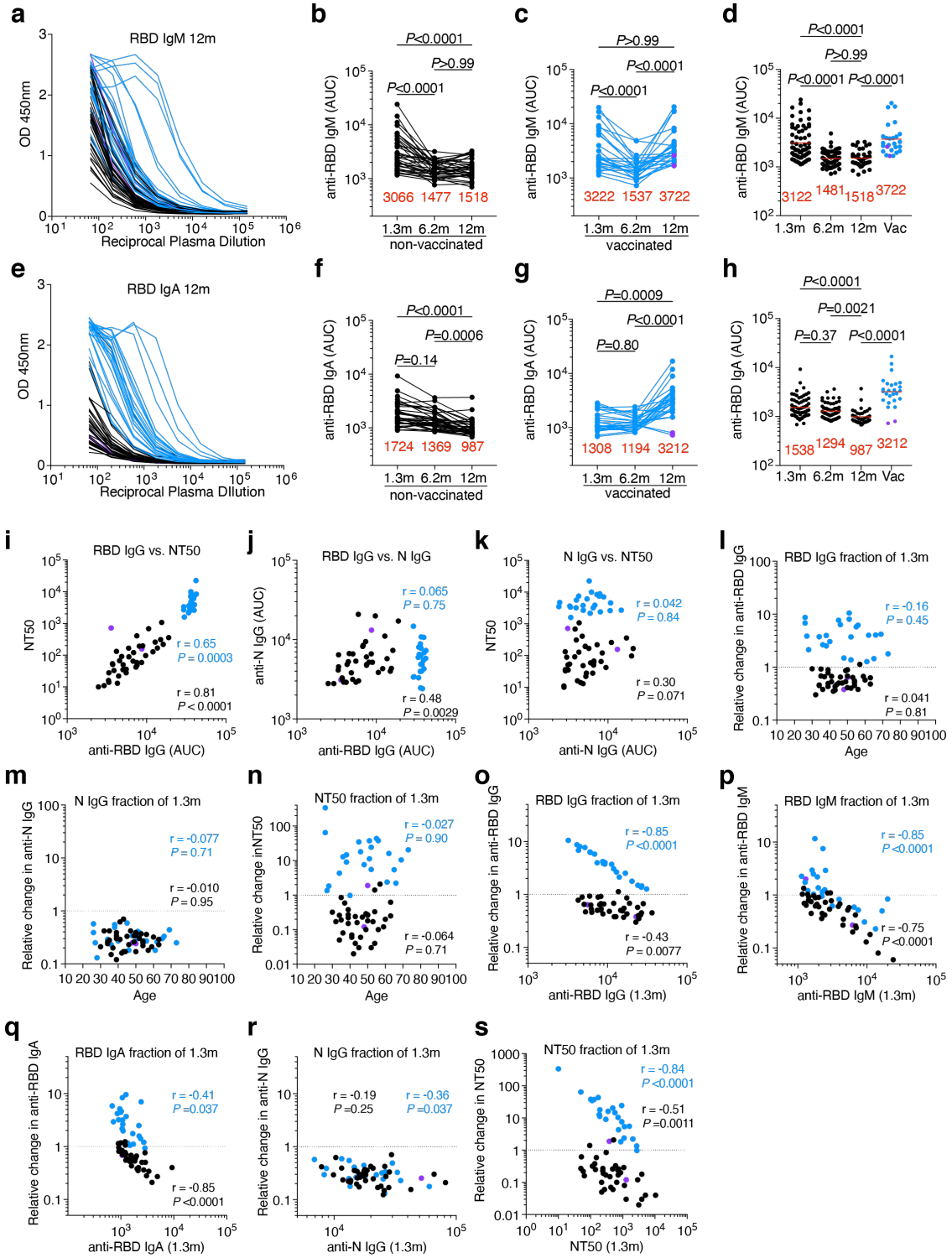

Extended Data Fig. 2: Plasma activity. a-h, ELISA results for plasma against SARS-CoV-2 RBD 12 months after infection (N=63). Non-vaccinated individuals are depicted with black circles

640 and lines, and vaccinated individuals are depicted in blue throughout. Two outlier individuals who
641 received their first dose of vaccine 24-48 hours before sample collection are depicted as purple
642 circles. **a-h,** IgM (**a-d**) and IgA (**e-h**) antibody binding to SARS-CoV-2 RBD 12 months after
643 infection. **a, e,** ELISA curves from non-vaccinated (black lines) individuals, as well as individuals
644 who received one or two doses (blue lines) of a COVID-19 mRNA vaccine (left panels). Area
645 under the curve (AUC) over time in non-vaccinated (**b** and **f**) and vaccinated individuals (**c** and **g**).
646 Lines in **b, c**, **f, g** connect longitudinal samples. **d, h,** Boxplots showing AUC values of all 63
647 individuals, as indicated. **i-r**, Correlation of serological parameters in non-vaccinated (black circles
648 and black statistics) and vaccinated (blue circles and blue statistics) individuals. Two individuals
649 who received their first dose of vaccine 24-48 hours before sample collection are depicted as purple
650 circles. **i-k**, Correlation of 12-month titers of anti- RBD IgG and NT50 (**i**), anti-RBD IgG and N
651 IgG (**j**), and anti-N IgG and NT50 (**k**). **l-n,** Correlation of remaining plasma titers at 12 months
652 (expressed as the fraction of 1.3-month titers on the Y axis) and participant age for anti-RBD IgG
653 (**l**), anti-N IgG (**m**), and NT50 (**n**). **o-s,** Correlation of remaining plasma titers at 12 months
654 (expressed as the relative change from 1.3-month titers on the Y axis) and initial plasma titers at
655 1.3 months for anti-RBD IgG (**o**), anti-RBD IgM (**p**), anti-RBD IgA (**q**), anti-N IgG (**m**), and NT50
656 (**s**). Statistical significance was determined using the Spearman correlation test for the non-
657 vaccinated and vaccinated subgroups independently. For **a-s** all experiments were performed at
658 least in duplicate.
659

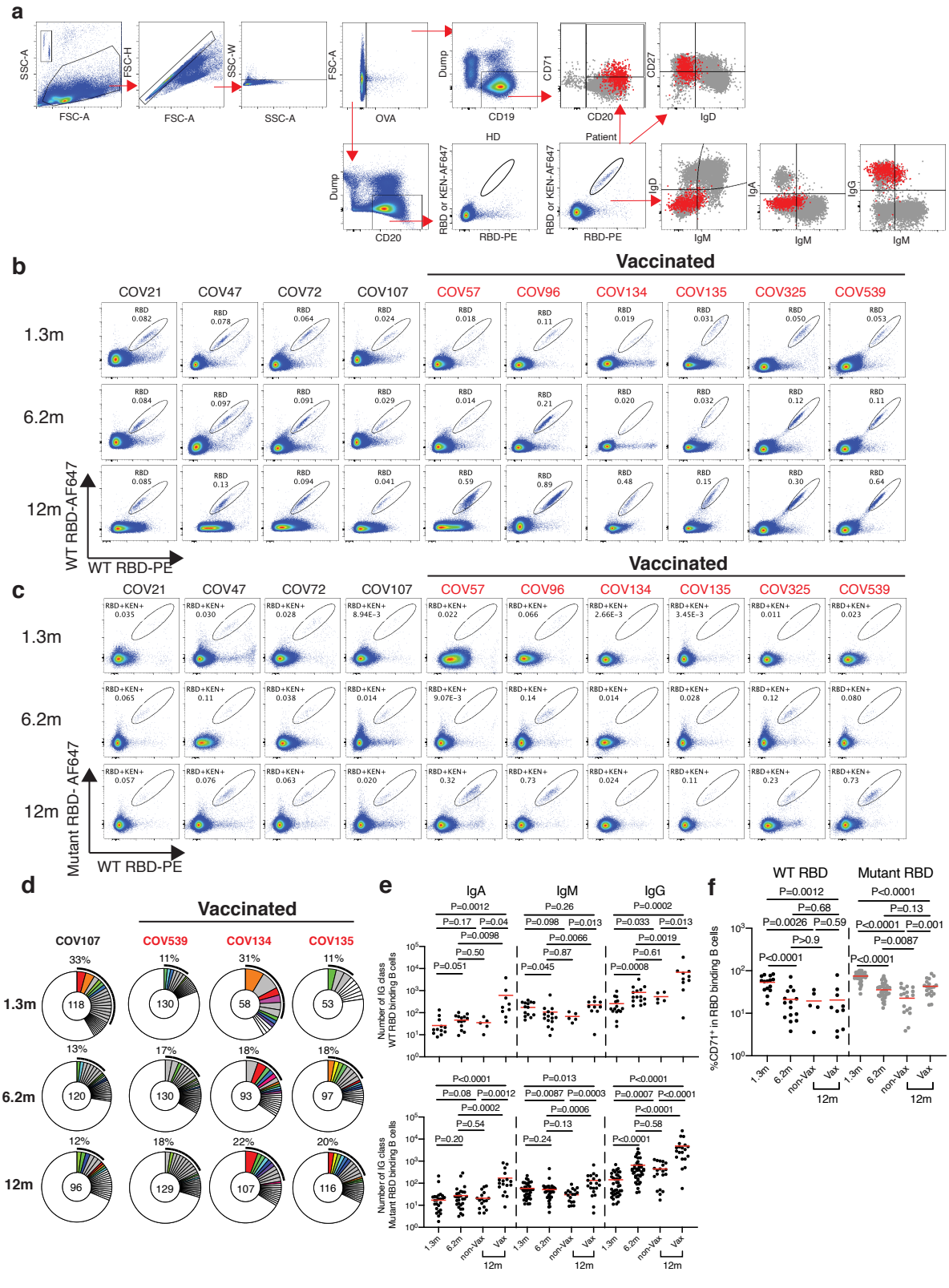
a
SSC-A
FSC-A
FSC-H
FSC-A
SSC-W
SSC-A
FSC-A
OVA
Dump
CD19
CD71
CD20
CD27
IgD
HD
Patient
Dump
CD20
RBD or KEN-AF647
RBD-PE
RBD or KEN-AF647
RBD-PE
IgD
IgM
IgA
IgM
IgG
IgM
b
Vaccinated
COV21
COV47
COV72
COV107
COV57
COV96
COV134
COV135
COV325
COV539
1.3m
6.2m
12m
WT RBD-AF647
WT RBD-PE
c
Vaccinated
COV21
COV47
COV72
COV107
COV57
COV96
COV134
COV135
COV325
COV539
1.3m
6.2m
12m
Mutant RBD- AF647
WT RBD-PE
d
Vaccinated
COV107
COV539
COV134
COV135
1.3m
6.2m
12m
33%
11%
31%
11%
118
130
58
53
13%
17%
18%
18%
120
130
93
97
12%
18%
22%
20%
96
129
107
116
e
IgA
IgM
IgG
P=0.0012
P=0.17
P=0.04
P=0.0098
P=0.50
P=0.051
P=0.26
P=0.098
P=0.013
P=0.0066
P=0.87
P=0.045
P=0.0002
P=0.033
P=0.013
P=0.0019
P=0.61
P=0.0008
Number of IG class WT RBD binding B cells
P<0.0001
P=0.08
P=0.0012
P=0.0002
P=0.54
P=0.20
P=0.013
P=0.0087
P=0.0003
P=0.0006
P=0.13
P=0.24
P<0.0001
P=0.0007
P<0.0001
P<0.0001
P=0.58
P<0.0001
Number of IG class Mutant RBD binding B cells
1.3m
6.2m
non-Vax
Vax
12m
f
WT RBD
Mutant RBD
P=0.0012
P=0.68
P=0.0026
P=0.59
P>0.9
P<0.0001
P<0.0001
P=0.13
P<0.0001
P=0.001
P=0.0087
P<0.0001
%CD71+ in RBD binding B cells
1.3m
6.2m
non-Vax
Vax
12m

660

661 **Extended Data Fig. 3: Flow cytometry. a,** Gating strategy. Gating was on singlets that were
662 $CD20^+$ or $CD19^+$ and CD3-CD8-CD16-Ova-. Anti-IgG, IgM, IgA, IgD, CD71 and CD27
663 antibodies were used for B cell phenotype analysis. Sorted cells were RBD-PE^+ and RBD/KEN-
664 $AF647^+$. **b and c,** Flow cytometry showing the percentage of RBD-double positive (**b**) and 647-
665 K417N/E484K/N501Y mutant RBD cross-reactive (**c**) memory B cells from 1.3 or 6- and 12-
666 months post-infection in 10 selected participants. **d**. as in Fig. 2c, Pie charts show the distribution
667 of antibody sequences from 4 individuals after 1.3 [3] (upper panel) or 6.2[4] months (middle panel)
668 or 12 months (lower panel). **e,** As in **b and c.** graph summarizes cell number (per 2 million B cells)
669 of immunoglobulin class of antigens binding memory B cells in samples obtained at 1.3, 6.2 and
670 12 months. **f,** same as in d**,** but summarizes percentage of CD71 positive activated antigen specific
671 B cells. Each dot is one individual. Red horizontal bars indicate mean values. Statistical
672 significance was determined using two-tailed Mann–Whitney U-tests.
673

674

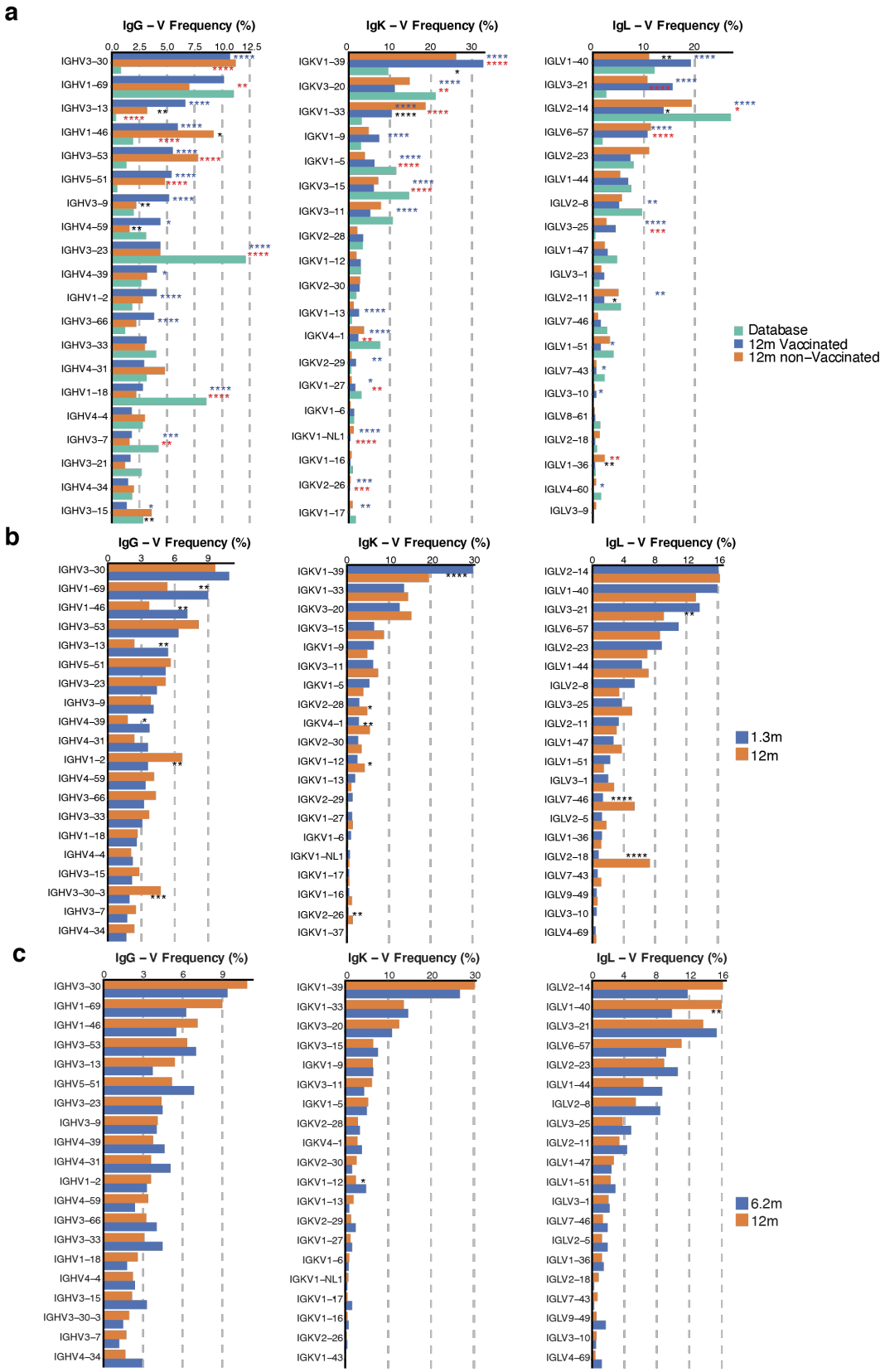
a
IgG – V Frequency (%)
IgK – V Frequency (%)
IgL – V Frequency (%)
Database
12m Vaccinated
12m non–Vaccinated
b
IgG – V Frequency (%)
IgK – V Frequency (%)
IgL – V Frequency (%)
1.3m
12m
c
IgG – V Frequency (%)
IgK – V Frequency (%)
IgL – V Frequency (%)
6.2m
12m

675

676 **Extended Data Fig. 4: Frequency distribution of human V genes.** Graph shows comparison of
677 the frequency distributions of human V genes of anti-SARS-CoV-2 antibodies from donors at 1.3[3],
678 6.2[4], 12 months after infection. **a,** Graph shows relative abundance of human IGVH genes
679 Sequence Read Archive accession SRP010970 (green), convalescent vaccinees (blue), and
680 convalescent non-vaccinees (orange). Statistical significance was determined by two-sided
681 binomial test. **b and c,** same as in **a**, but showing comparison between antibodies from donors at
682 1.3 months[3] (**b**), 6.2 month[4] (**c**), and 12 months after infection.
683

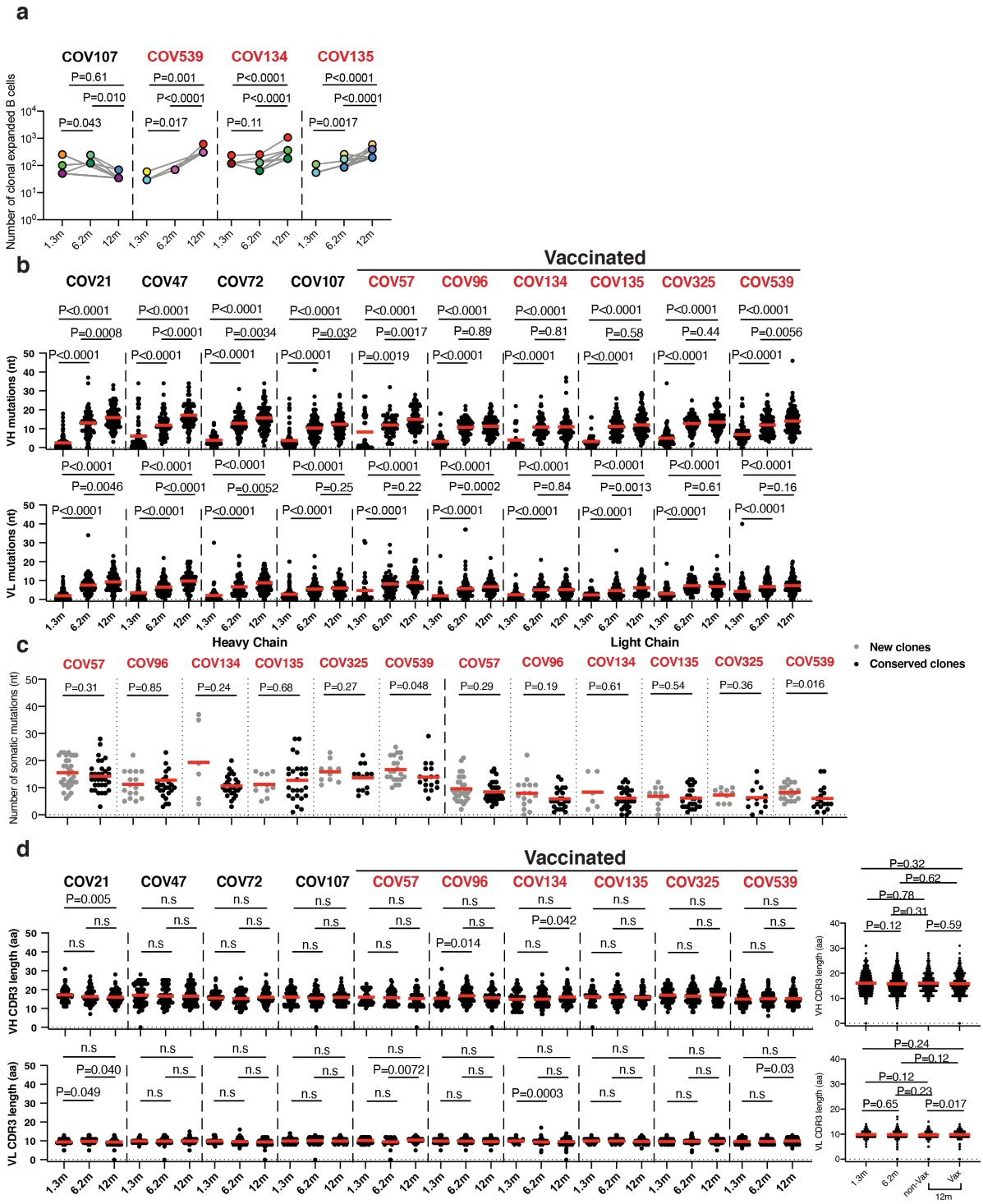

Extended Data Fig. 5: Analysis of anti-RBD antibodies. a, as in Fig. 2e, graph shows number of clonally expanded B cells (per 10 million B cells) at both time points from four individuals.

688 Cells belonging the same clone are marked in the same color. Statistical significance was
689 determined using Wilcoxon matched-pairs signed rank tests. Vaccinees are marked in red. **b.**
690 Number of somatic nucleotide mutations in the IGVH (top) and IGVL (bottom) in antibodies
691 obtained after 1.3 or 6.2 or 12 months from the indicated individual. **c.** same as **b**, but graphs show
692 comparison between new clones and conserved clones in 6 vaccinated convalescent individuals at
693 12 months after infection. **d.** The amino acid length of the CDR3s at the IGVH and IGVL for each
694 individual. Right panel shows all antibodies combined. The horizontal bars indicate the mean.
695 Statistical significance was determined using two-tailed Mann–Whitney U-tests.
696

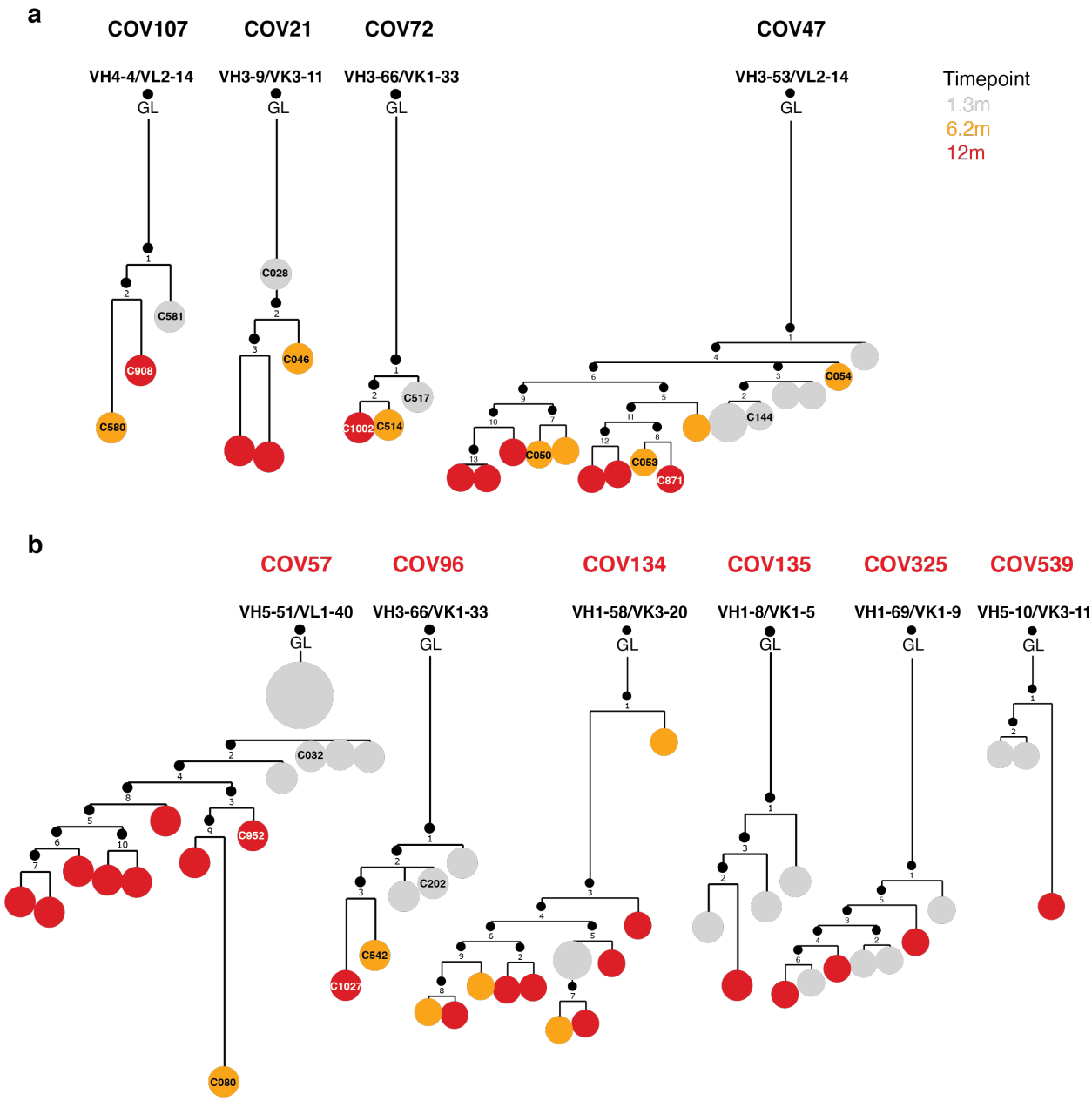

Extended Data Fig. 6: Evolution of anti-SARS-CoV-2 RBD antibody clone. Clonal evolution of RBD-binding memory B cells from ten convalescent individuals, **a**, phylogenetic tree graph shows clones from convalescent non-vaccinees, **b**, same as **a**, but from convalescent vaccinees. Numbers refer to mutations compared to the preceding vertical node. Colors indicate timepoint;

703 grey, orange and red represent 1.3, 6 and 12 months respectively, black dots indicate inferred

704 nodes, and size is proportional to sequence copy number; GL = germline sequence.

705

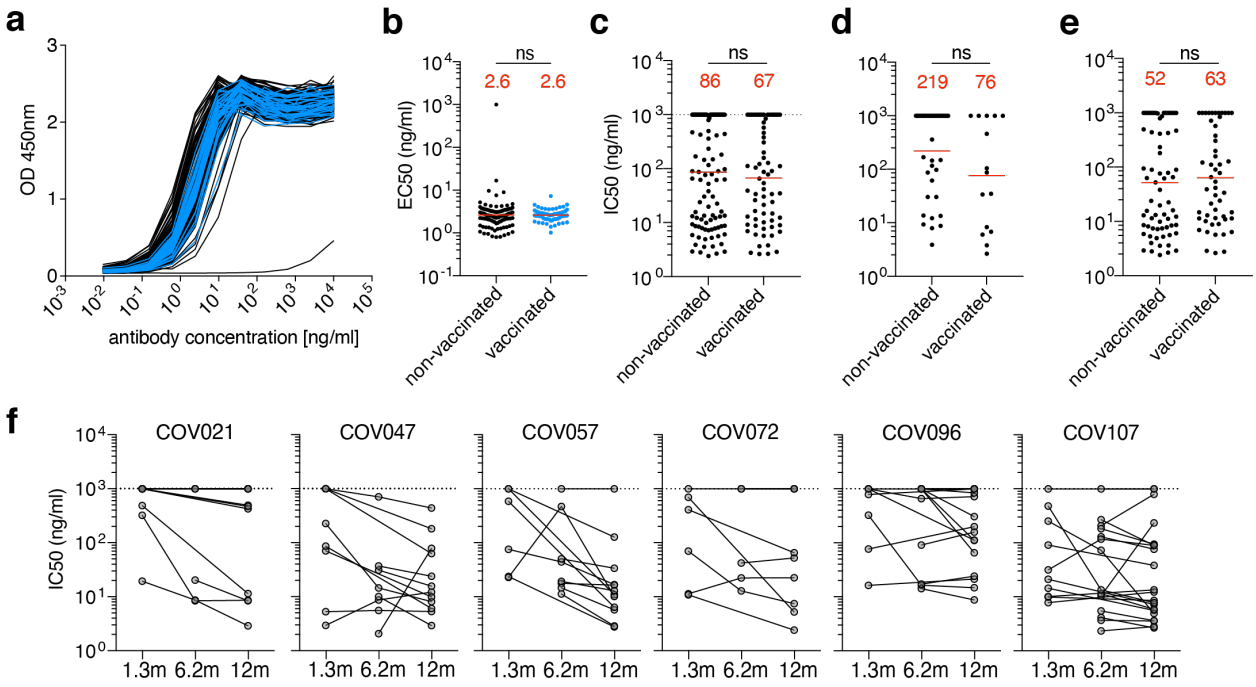

706

707

708 **Extended Data Fig. 7: Neutralization of WT RBD pseudovirus by mAbs. A,b,** Binding curves
709 (**a**) and EC50 dot plot (**b**) of mAbs isolated from non-vaccinated (black curves and dots) and from
710 vaccinated (blue curves and dots) convalescents individuals 12 months after infection. **c-e,** IC_{50}
711 values of mAbs isolated 12 months after infection from non-vaccinated and vaccinated individuals.
712 **c** shows all 12-month antibodies irrespective of clonality, **d** shows singlets only, and **e** shows only
713 antibodies belonging to a clone or shared over time. Statistical significance was determined using
714 Mann-Whitney test. Geometric mean IC_{50} is indicated in red. **f,** IC_{50} values of shared clones of
715 mAbs cloned from B-cells from the initial 1.3- and 6.2, as well as 12-month follow-up visit,
716 divided by participant, as indicated. Lines connect clonal antibodies shared between time points.
717 Antibodies with IC50>1000ng/ml are plotted at 1000 ng/ml. Average IC_{50} values of two
718 independent experiments are shown.

719

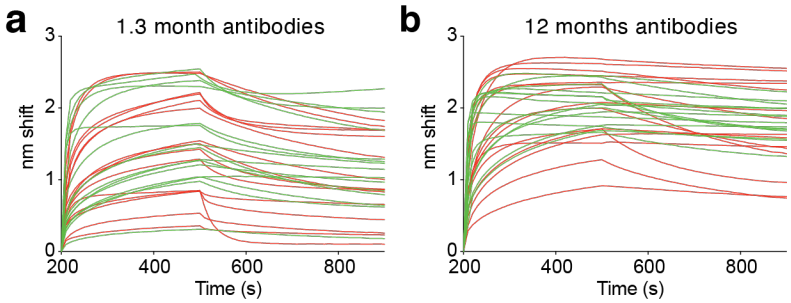

Extended Data Fig. 8: Biolayer interferometry affinity measurements. a-b, Graphs depict affinity measurements of neutralizing (green) and non-neutralizing (red) antibodies isolated 1.3 months (**a)** or 12 months (**b)** after infection.

726

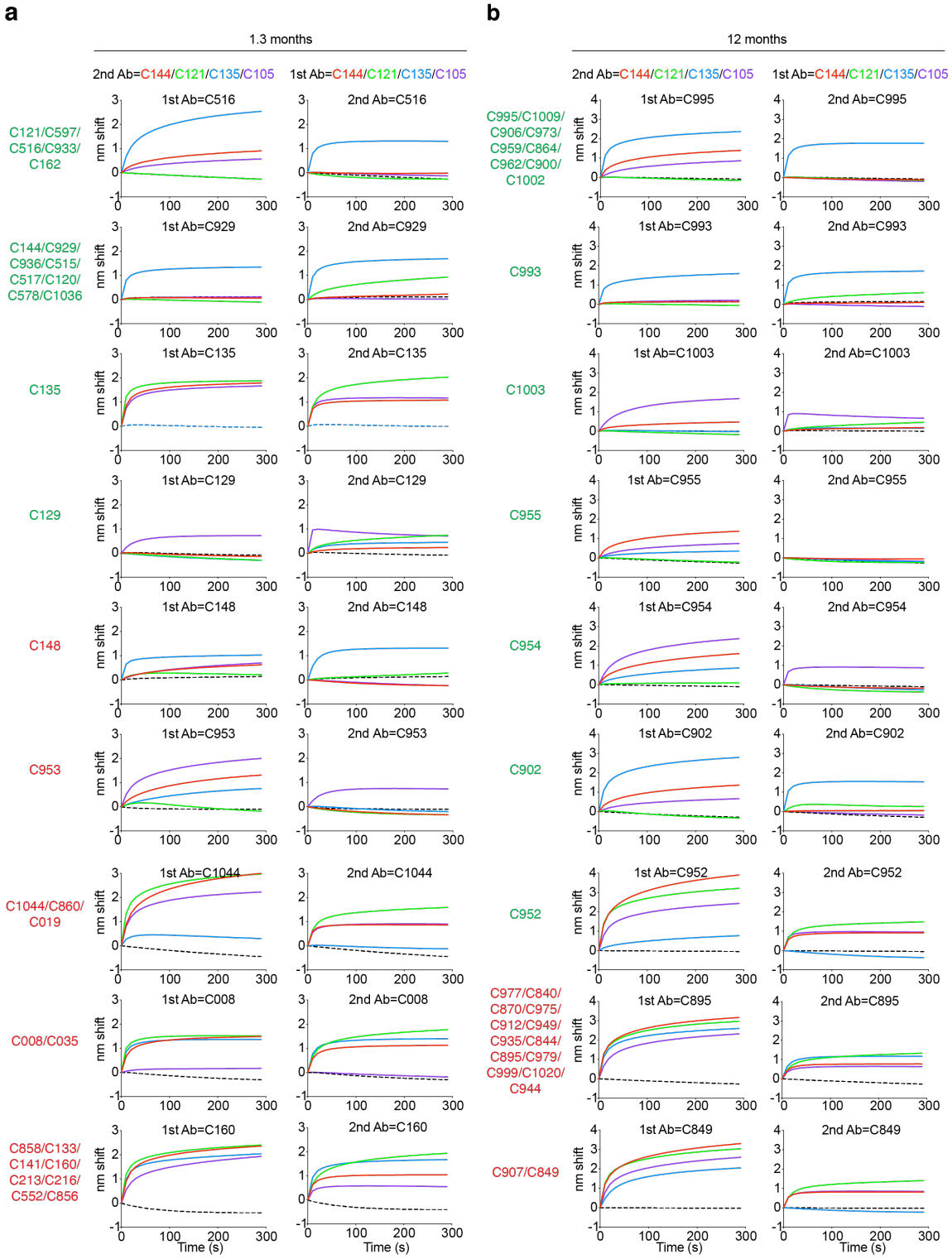
a
1.3 months
2nd Ab=C144/C121/C135/C105
1st Ab=C144/C121/C135/C105
C121/C597/C516/C933/C162
1st Ab=C516
2nd Ab=C516
C144/C929/C936/C515/C517/C120/C578/C1036
1st Ab=C929
2nd Ab=C929
C135
1st Ab=C135
2nd Ab=C135
C129
1st Ab=C129
2nd Ab=C129
C148
1st Ab=C148
2nd Ab=C148
C953
1st Ab=C953
2nd Ab=C953
C1044/C860/C019
1st Ab=C1044
2nd Ab=C1044
C008/C035
1st Ab=C008
2nd Ab=C008
C858/C133/C141/C160/C213/C216/C552/C856
1st Ab=C160
2nd Ab=C160
nm shift
Time (s)
b
12 months
2nd Ab=C144/C121/C135/C105
1st Ab=C144/C121/C135/C105
C995/C1009/C906/C973/C959/C864/C962/C900/C1002
1st Ab=C995
2nd Ab=C995
C993
1st Ab=C993
2nd Ab=C993
C1003
1st Ab=C1003
2nd Ab=C1003
C955
1st Ab=C955
2nd Ab=C955
C954
1st Ab=C954
2nd Ab=C954
C902
1st Ab=C902
2nd Ab=C902
C952
1st Ab=C952
2nd Ab=C952
C977/C840/C870/C975/C912/C949/C935/C844/C895/C979/C999/C1020/C944
1st Ab=C895
2nd Ab=C895
C907/C849
1st Ab=C849
2nd Ab=C849
nm shift
Time (s)

727

728 **Extended Data Fig. 9: Biolayer interferometry antibody competition experiment. a-b,** Anti-
729 SARS-CoV-2 RBD antibodies isolated 1.3 (**a**) or 12 months (**b**) after infection were assayed for
730 competition with structurally characterized anti-RBD antibodies by biolayer interferometry
731 experiments as in Fig 4a. Graphs represent the binding of the second antibody (2nd Ab) to
732 preformed first antibody (1st Ab)–RBD complexes. Dotted line denotes when 1st Ab and 2nd Ab
733 are the same. For each antibody group identified in Fig 4c the left graphs represent the binding of
734 the class-representative C144, C121, C135 or C105 [3,20](2nd Ab) to the candidate antibody (1st
735 Ab)-RBD complex. The right graphs represent the binding of the candidate antibody (2nd Ab) to
736 the complex of C144-RBD, C121-RBD, C135-RBD or C105-RBD (1st Ab). Antibodies belonging
737 to the same groups are indicated to the left of the respective curves.
738

739 **Supplementary Tables**

740 **Supplementary Table 1: Cohort summary**

741 **Supplementary Table 2: Individual participant characteristics**

742 **Supplementary Table 3: Antibody sequences from patients is provided as a separate Excel**
743 **file.**

744 **Supplementary Table 4: Sequences, half maximal effective concentrations (EC50s) and**
745 **inhibitory concentrations (IC50s) of the cloned monoclonal antibodies is provided as a**
746 **separate Excel file.**

747 **Supplementary Table 5: Binding and Neutralization activity of mAbs against mutant**
748 **SARS-CoV-2 pseudoviruses.**

749 **Supplementary Table 6: Neutralization activity of mAbs against mutant SARS-CoV-2**
750 **pseudoviruses - Random potently neutralizing antibodies isolated at 1.3 and 12 months**

751 **Supplementary Table 7: Antibody affinities and neutralization - Clonal pairs isolated at 1.3**
752 **and 12 months**

753 **Supplementary Table 8: Neutralization activity of mAbs against mutant SARS-CoV-2**
754 **pseudoviruses - Clonal pairs isolated at 1.3 and 12 months.**

755

Reference:

1 Davies, N. G. *et al.* Estimated transmissibility and impact of SARS-CoV-2 lineage B.1.1.7 in England. *Science* **372**, doi:10.1126/science.abg3055 (2021).

2 Wang, Z. *et al.* mRNA vaccine-elicited antibodies to SARS-CoV-2 and circulating variants. *Nature* **592**, 616-622, doi:10.1038/s41586-021-03324-6 (2021).

3 Robbiani, D. F. *et al.* Convergent antibody responses to SARS-CoV-2 in convalescent individuals. *Nature* **584**, 437-442, doi:10.1038/s41586-020-2456-9 (2020).

4 Gaebler, C. *et al.* Evolution of antibody immunity to SARS-CoV-2. *Nature* **591**, 639-644, doi:10.1038/s41586-021-03207-w (2021).

5 Goel, R. R. *et al.* Distinct antibody and memory B cell responses in SARS-CoV-2 naive and recovered individuals following mRNA vaccination. *Sci Immunol* **6**, doi:10.1126/sciimmunol.abi6950 (2021).

6 Saadat, S. *et al.* Binding and Neutralization Antibody Titers After a Single Vaccine Dose in Health Care Workers Previously Infected With SARS-CoV-2. *JAMA* **325**, 1467-1469, doi:10.1001/jama.2021.3341 (2021).

7 Krammer, F. *et al.* Antibody Responses in Seropositive Persons after a Single Dose of SARS-CoV-2 mRNA Vaccine. *N Engl J Med* **384**, 1372-1374, doi:10.1056/NEJMc2101667 (2021).

8 Reynolds, C. J. *et al.* Prior SARS-CoV-2 infection rescues B and T cell responses to variants after first vaccine dose. *Science*, doi:10.1126/science.abh1282 (2021).

9 Muecksch, F. *et al.* Development of potency, breadth and resilience to viral escape mutations in SARS-CoV-2 neutralizing antibodies. *bioRxiv*, doi:10.1101/2021.03.07.434227 (2021).

10 Schmidt, F. *et al.* Measuring SARS-CoV-2 neutralizing antibody activity using pseudotyped and chimeric viruses. *J Exp Med* **217**, doi:10.1084/jem.20201181 (2020).

11 Tegally, H. *et al.* Detection of a SARS-CoV-2 variant of concern in South Africa. *Nature* **592**, 438-443, doi:10.1038/s41586-021-03402-9 (2021).

12 West, A. P. *et al.* Detection and characterization of the SARS-CoV-2 lineage B.1.526 in New York. *bioRxiv*, 2021.2002.2014.431043, doi:10.1101/2021.02.14.431043 (2021).

13 Inoue, T. *et al.* Exit from germinal center to become quiescent memory B cells depends on metabolic reprograming and provision of a survival signal. *J Exp Med* **218**, doi:10.1084/jem.20200866 (2021).

14 Viant, C. *et al.* Antibody Affinity Shapes the Choice between Memory and Germinal Center B Cell Fates. *Cell* **183**, 1298-1311 e1211, doi:10.1016/j.cell.2020.09.063 (2020).

15 Stamatatos, L. *et al.* mRNA vaccination boosts cross-variant neutralizing antibodies elicited by SARS-CoV-2 infection. *Science*, doi:10.1126/science.abg9175 (2021).

16 Sokal, A. *et al.* Maturation and persistence of the anti-SARS-CoV-2 memory B cell response. *Cell* **184**, 1201-1213 e1214, doi:10.1016/j.cell.2021.01.050 (2021).

17 Sakharkar, M. *et al.* Prolonged evolution of the human B cell response to SARS-CoV-2 infection. *Sci Immunol* **6**, doi:10.1126/sciimmunol.abg6916 (2021).

18 Brouwer, P. J. M. *et al.* Potent neutralizing antibodies from COVID-19 patients define multiple targets of vulnerability. *Science* **369**, 643-650, doi:10.1126/science.abc5902 (2020).

19 Rogers, T. F. *et al.* Isolation of potent SARS-CoV-2 neutralizing antibodies and protection from disease in a small animal model. *Science* **369**, 956-963, doi:10.1126/science.abc7520 (2020).

20 Barnes, C. O. *et al.* SARS-CoV-2 neutralizing antibody structures inform therapeutic strategies. *Nature* **588**, 682-687, doi:10.1038/s41586-020-2852-1 (2020).

21 Hoffmann, M. *et al.* SARS-CoV-2 Cell Entry Depends on ACE2 and TMPRSS2 and Is Blocked by a Clinically Proven Protease Inhibitor. *Cell* **181**, 271-280 e278, doi:10.1016/j.cell.2020.02.052 (2020).

22 Greaney, A. J. *et al.* Mutational escape from the polyclonal antibody response to SARS-CoV-2 infection is largely shaped by a single class of antibodies. *bioRxiv*, doi:10.1101/2021.03.17.435863 (2021).

23 Weisblum, Y. *et al.* Escape from neutralizing antibodies by SARS-CoV-2 spike protein variants. *Elife* **9**, doi:10.7554/eLife.61312 (2020).

24 Elsner, R. A. & Shlomchik, M. J. Germinal Center and Extrafollicular B Cell Responses in Vaccination, Immunity, and Autoimmunity. *Immunity* **53**, 1136-1150, doi:10.1016/j.immuni.2020.11.006 (2020).

25 Lau, A. W. & Brink, R. Selection in the germinal center. *Curr Opin Immunol* **63**, 29-34, doi:10.1016/j.coi.2019.11.001 (2020).

26 Victora, G. D. & Nussenzweig, M. C. Germinal centers. *Annu Rev Immunol* **30**, 429-457, doi:10.1146/annurev-immunol-020711-075032 (2012).

27 Inoue, T., Moran, I., Shinnakasu, R., Phan, T. G. & Kurosaki, T. Generation of memory B cells and their reactivation. *Immunol Rev* **283**, 138-149, doi:10.1111/imr.12640 (2018).

28 Taylor, J. J., Pape, K. A., Steach, H. R. & Jenkins, M. K. Humoral immunity. Apoptosis and antigen affinity limit effector cell differentiation of a single naive B cell. *Science* **347**, 784-787, doi:10.1126/science.aaa1342 (2015).

29 McKean, D. *et al.* Generation of antibody diversity in the immune response of BALB/c mice to influenza virus hemagglutinin. *Proc Natl Acad Sci U S A* **81**, 3180-3184, doi:10.1073/pnas.81.10.3180 (1984).

30 Petersen, M. S. *et al.* SARS-CoV-2 natural antibody response persists up to 12 months in a nationwide study from the Faroe Islands. *medRxiv*, 2021.2004.2019.21255720, doi:10.1101/2021.04.19.21255720 (2021).

31 Li, C. *et al.* Twelve-month specific IgG response to SARS-CoV-2 receptor-binding domain among COVID-19 convalescent plasma donors in Wuhan. *bioRxiv*, 2021.2004.2005.437224, doi:10.1101/2021.04.05.437224 (2021).

32 Turner, J. *et al.* SARS-CoV-2 mRNA vaccines induce a robust germinal centre reaction in humans. *Research Square*, doi:https://www.researchsquare.com/article/rs-310773/v1 (2021).

33 Greaney, A. J. *et al.* The SARS-CoV-2 mRNA-1273 vaccine elicits more RBD-focused neutralization, but with broader antibody binding within the RBD. *bioRxiv*, doi:10.1101/2021.04.14.439844 (2021).

34 Wang, Z. *et al.* Enhanced SARS-CoV-2 neutralization by dimeric IgA. *Sci Transl Med* **13**, doi:10.1126/scitranslmed.abf1555 (2021).

35 Schoof, M. *et al.* An ultrapotent synthetic nanobody neutralizes SARS-CoV-2 by stabilizing inactive Spike. *Science* **370**, 1473-1479, doi:10.1126/science.abe3255 (2020).

843 36 De Gasparo, R. *et al.* Bispecific IgG neutralizes SARS-CoV-2 variants and prevents escape
844 in mice. *Nature*, doi:10.1038/s41586-021-03461-y (2021).
845 37 Xu, J. *et al.* Multimeric nanobodies from camelid engineered mice and llamas potently
846 neutralize SARS-CoV-2 variants. *bioRxiv*, doi:10.1101/2021.03.04.433768 (2021).
847 38 Wu, F. *et al.* A new coronavirus associated with human respiratory disease in China.
848 *Nature* **579**, 265-269, doi:10.1038/s41586-020-2008-3 (2020).
849 39 Chomczynski, P. & Sacchi, N. Single-step method of RNA isolation by acid guanidinium
850 thiocyanate-phenol-chloroform extraction. *Analytical biochemistry* **162**, 156-159,
851 doi:10.1006/abio.1987.9999 (1987).
852 40 DeAngelis, M. M., Wang, D. G. & Hawkins, T. L. Solid-phase reversible immobilization for
853 the isolation of PCR products. *Nucleic Acids Res* **23**, 4742-4743,
854 doi:10.1093/nar/23.22.4742 (1995).
855 41 Grifoni, A. *et al.* Targets of T Cell Responses to SARS-CoV-2 Coronavirus in Humans with
856 COVID-19 Disease and Unexposed Individuals. *Cell* **181**, 1489-1501 e1415,
857 doi:10.1016/j.cell.2020.05.015 (2020).
858 42 Amanat, F. *et al.* A serological assay to detect SARS-CoV-2 seroconversion in humans.
859 *Nat Med* **26**, 1033-1036, doi:10.1038/s41591-020-0913-5 (2020).
860 43 Barnes, C. O. *et al.* Structures of Human Antibodies Bound to SARS-CoV-2 Spike Reveal
861 Common Epitopes and Recurrent Features of Antibodies. *Cell* **182**, 828-842 e816,
862 doi:10.1016/j.cell.2020.06.025 (2020).
863 44 Gupta, N. T. *et al.* Change-O: a toolkit for analyzing large-scale B cell immunoglobulin
864 repertoire sequencing data. *Bioinformatics (Oxford, England)* **31**, 3356-3358,
865 doi:10.1093/bioinformatics/btv359 (2015).
866 45 Soto, C. *et al.* High frequency of shared clonotypes in human B cell receptor repertoires.
867 *Nature* **566**, 398-402, doi:10.1038/s41586-019-0934-8 (2019).
868 46 Guo, Y., Chen, K., Kwong, P. D., Shapiro, L. & Sheng, Z. cAb-Rep: A Database of Curated
869 Antibody Repertoires for Exploring Antibody Diversity and Predicting Antibody
870 Prevalence. *Front Immunol* **10**, 2365, doi:10.3389/fimmu.2019.02365 (2019).
871 47 Kyte, J. & Doolittle, R. F. A simple method for displaying the hydropathic character of a
872 protein. *J Mol Biol* **157**, 105-132, doi:10.1016/0022-2836(82)90515-0 (1982).
873 48 Guy, H. R. Amino acid side-chain partition energies and distribution of residues in
874 soluble proteins. *Biophysical journal* **47**, 61-70, doi:10.1016/S0006-3495(85)83877-7
875 (1985).
876 49 DeWitt, W. S. *et al.* A Public Database of Memory and Naive B-Cell Receptor Sequences.
877 *PLoS One* **11**, e0160853, doi:10.1371/journal.pone.0160853 (2016).
878 50 Abascal, F., Zardoya, R. & Telford, M. J. TranslatorX: multiple alignment of nucleotide
879 sequences guided by amino acid translations. *Nucleic Acids Res* **38**, W7-13,
880 doi:10.1093/nar/gkq291 (2010).
881 51 Lefranc, M. P. IMGT, the International ImMunoGeneTics Information System. *Cold*
882 *Spring Harb Protoc* **2011**, 595-603, doi:10.1101/pdb.top115 (2011).
883 52 DeWitt, W. S., 3rd, Mesin, L., Victora, G. D., Minin, V. N. & Matsen, F. A. t. Using
884 Genotype Abundance to Improve Phylogenetic Inference. *Mol Biol Evol* **35**, 1253-1265,
885 doi:10.1093/molbev/msy020 (2018).
886